nature portfolio

# Peer Review File

# Targeting chaperone-mediated autophagy inhibits properties of glioblastoma stem cells and restores anti-tumor immunity

Corresponding Author: Dr Tianzhi Huang

**This file contains all reviewer reports in order by version, followed by all author rebuttals in order by version.**

**Attachments originally included by the reviewers as part of their assessment can be found at the end of this file.**

Version 0:

Reviewer comments:

Reviewer #1

(Remarks to the Author)
Li, Sheng and Li et al studied how chaperone-mediated autophagy (CMA) affects the tumor activity of glioblastoma (GBM). Using multiple lines of evidence, the authors identified MST4 as an interaction partner of LAMP2A, the only known lysosomal CMA receptor, and that its phosphorylation of LAMP2A enhanced LAMP2A's stability in the lysosome, CMA activity and GBM stem cell tumorigenicity. Next, using mouse models, the authors found that inhibiting CMA activity through knockdown of LAMP2A or MST4 led to reduced tumor growth and higher survival, which was mediated by T cell immune response. Mechanistically, the authors showed that CMA enhanced tumor activity via suppression of TSC1/2 proteins, which are negative regulators of the mTORC1 pathway, and via suppression of TET3 protein, which upregulates the cGAS-STING pathway via DNA demethylation. Finally, the authors showed the effectiveness of a GBM treatment strategy that combined CMA inhibition with radiotherapy and immune checkpoint therapy.

I am not qualified to comment on the biological novelty of the study. Besides that, the study is an impressive endeavor, as evidenced by the large amount of effort that has gone into it. I especially appreciate that the authors were able to verify their findings in GBM patients. At the editor's discretion, I think the study contains enough information for two separate papers.

Major comments:
1. The authors have not made their code available, especially for the RNA-seq analyses, for review.
2. Could the authors discuss how the GSC cell line 23 still shows higher activation of CMA compared to non-GSC cell lines (Fig 1), despite the former's very low expression of MST4 (Fig 5a)?
3. Did the authors use the same data for the red survival curve in Fig 7j and the black survival curve in Fig 10d? They look quite similar.
4. The authors should provide information on the characteristics of the 83 patients analyzed in Fig 11 (similar to the Table 1 in clinical papers). How did the authors take into account potential confounders when analyzing the clinical samples? Did the patients have any noteworthy co-morbidities?

Minor comments:
1. What statistical test did the authors use for the sphere-forming frequency analyses (those like Fig 1f). Why do those plots always have upside down triangles at y-values < -3 and x-values = 20 and 50?
2. Fig 1a, d: the error bars in the quantification of puncta per cell look unusually small compared to the variance of the data, and the error bars of different groups look almost identical to one another.
3. Is Fig 1c missing the results after treatment with NH4Cl? It was mentioned in the figure caption and the text (lines 114, 115).
4. Fig 1d: the left images show cell lines M83 and 23, while the right plot shows cell lines M83 and 456. Was this intentional?
5. Fig 2: did the author use LN as the protease inhibitor?
6. Fig 4b-d, g-h: the authors should also show the P-values comparing the blue and black data.
7. Fig 5c: please indicate the P-values on the legend like Fig 4d.
8. Fig 6a: the x-axis should say "0.00" instead of "-0.00".
9. Fig 7j: the authors should show the P-value comparing the green and blue lines.

10. Lines 549 and 554: did the authors mean GSCs instead of “CSCs”?
11. Line 720: “quired” typo.

Reviewer #2

(Remarks to the Author)
This study by Li et al. explores the role of the MST4-LAMP2A axis in regulating chaperone-mediated autophagy (CMA) and its impact on glioblastoma stem cell (GSC) proliferation. The authors report elevated levels of LAMP2A in patient-derived GSCs and demonstrate that LAMP2A downregulation in glioma cell lines reduces GSC proliferation in vitro while improving survival in orthotopic immunodeficient mouse models. Mechanistically, they identify MST4 as a key regulator that phosphorylates LAMP2A, enhancing its stability in GSC lysosomes and promoting mTORC1 activation through the degradation of its negative regulators, TSC1 and TSC2. Therapeutically, the study links this pathway to immune evasion via suppression of the cGAS-STING axis and shows that inhibiting CMA synergizes with anti-PD-1 therapy in a GL261 syngeneic model. Overall, the paper provides a comprehensive mechanism for CMA regulation and presents a strong case for targeting CMA as a potential therapeutic strategy for glioblastoma.

Major points:
-The paper is very comprehensive with the introduction explaining the key players of the mechanism behind CMA modulation for GSCs. The results flow well with logical progression of the rationale behind targeting MST4 or LAMP2A
-Given recent studies that have highlighted the importance of efferocytosis in the tumor microenvironment with autophagy, the authors should mention this process as it is directly impacted by their proposed therapy. This would also strengthen the study’s scope of mechanism in that it would functionally incorporate myeloid cells into the pathways described
-GL261 is a very immunogenic model that is now out of favor compared to more resistant lines such as CT-2A and SB28. The preclinical orthotopic data could be strengthened by showing survival studies with these additional models
-This study could be significantly strengthened by including further immunophenotyping beyond CD8+ T cells (e.g. Tregs, TAMs, MDSCs). By characterizing the immune microenvironment further (in both human tissue samples as well as in the syngeneic model), the role of CMA in impacting the immune milieu could be better understood. This would especially be helpful for expanding on the overlap with cGAS-STING and this strategy synergizing with anti-PD-1 as shown in the study.

Minor points:
-Please undergo mechanical revision for minor errors (i.e. line 51 Prior study has identified…)

Reviewer #3

(Remarks to the Author)
In this study, Li et al show that CMA is upregulated in patient-derived glioblastoma stem cells characterized by a notable increase in the levels of the CMA receptor, lysosome-associated membrane protein type 2A (LAMP2A). Moreover, their experiments delineate an MST4-LAMP2A signaling pathway that modulates CMA activity and facilitates tumor initiation and immune escape of GSCs.

The results describing that CMA and LAMP2A are increased in patient-derived glioblastoma stem cells and associated with poor patient survival have been previously described (Auzmendi-iriarte et al Cancer Research). Similarly, that study described that CMA activity promotes tumor initiation and progression and revealed immune escape and metabolism as critical processes involved on them. Indeed, the OMIC data used in the study of Li et al were generated on the Auzmendi-iriarte study. Although the study of Li et al went deeper in the description of the molecular mechanisms underlying CMA activity, it does not present enough novelty and relevance to be published in Nature Communications. I I think the manuscript suits better in a specific journal of autophagy.

Reviewer #4

(Remarks to the Author)
In the manuscript, the authors describe a novel mechanism of CMA regulation by stabilization of LAMP2A in the lysosome through its phosphorylation by MTS4. They also state that they have described two CMA targets that are implicated in GSC tumorigenicity: TCS1/2, implicated in mTOR1 pathway, and TET3, implicated in cGAS-STING pathway. Nevertheless, they don’t clearly demonstrate that TET3 and TSC1/2 are CMA substrates, and that the effects they see in GSC tumorigenicity changes are only due to CMA modulation and not to macroautophagy. Importantly, there is not clear link between CMA regulation, effects they see in GSC tumorigenicity and the possible substrates, as they try to show this link only using a pharmacological modulator of CMA which might be none specific and also induce other cellular stress mechanisms.

The authors should address several major points to improve their study and meet the standards of the journal.

· The authors state in the introduction: “MST4 is recognized for phosphorylating ATGB4, thereby initiating macroautophagy, which enhances cell survival and tumorogenic potential of GSCs”. However, when they regulate MST4 levels, they only attribute changes in GCS tumorigenicity to changes in CMA without showing if also levels of macroautophagy are changed (LC3 flux). They must show if macroautophagy is implicated in MST4 regulation of tumorgenicity.

· Authors do not follow all the known guidelines to validate their potential CMA substrates, therefore, they are not showing that MST4 and TET3 are CMA substrates (doi.org/10.1080/15548627.2020.1797280).

· Authors must show the quality of lysosome preparations. They should show enrichment of LAMP1 or LAMP2A in the lysosome lysates vs whole cell lysates by WesternBlot. Moreover, they must show the quality of the lysosomal preparations, showing absence of mitochondrial and cytosolic markers in their Western-blot with lysosomal preparations.

· Authors must clearly demonstrate that lysosomes are CMA competent: they should see an increase in HSC70 and not only in LAMP2A levels in WB to conclude there's an activation of CMA. They should corroborate that those CMA competent lysosomes have increased phosphorylated LAMP2A when modifying MST4 levels.

· TCS1/2 is a known regulator of macroautophagy. Authors should prove that regulation of TCS1/2 does not alter macroautophagy levels, so that the effects on GCS that they see in tumorigenicity are caused only by CMA regulation.

· Besides all the above recommendations to validate CMA substrates, authors also should validate that TET3 expression they see is due to changes in protein levels and not due to gene expression (measuring mRNA levels).

· If authors are able to demonstrate that TET3 and TCS1/2 are CMA substrates, they should show if the increased stability of the phosphorylated LAMP2A at the lysosomal membrane is a common mechanism among other types of cells, not only in GSCs. They should include a model where CMA is downregulated ( for example an aging model) and test whether they can restore CMA by introducing the phosphomimic version they use.

· During the whole manuscript, authors are trying to point out the relevance of CMA for GSC tumorigenicity and proliferative potential. They are trying to prove that by performing several in vitro and in vivo analysis with different lines of human GSC. Nevertheless, when they test in the in vivo model if LAMP2A or MTS4 regulation in tumor cells changes the immune response to the tumor (Figure 7), they use GB mouse cells, even if they have the tools to do it with the modified GSC. They also use GB mouse cells when studying the effects of IR therapy and anti-PD1 therapy in the in vivo model (Figure 10). Authors should show the results of immune regulation effects with the human GCS lines with the corresponding genetic modifications.

· The inhibitor PPD is used arbitrarily and without context. To improve the quality of the work, authors should show the link, if any, between the phosphorylation of LAMP2A and the modulation of the CMA activity by PPD.

· Supplementary Fig. 1E-H- Authors show some redundant analyses, previously published by other authors (Auzmendi-Iriarte et al., 2022) DOI: 10.1158/0008-5472.CAN-21-2161

· Introduction. Authors should enhance the quality of the documentation for the work since their claims are poorly substantiated. Fox example, authors state in line 72 that "the regulatory mechanisms and 73 physiological roles of CMA remain poorly understood", which shows a lack of documentation for the study. To improve the introduction section, they could add different works and reviews on the physiological significance of CMA (doi:10.1038/s41580-018-0001-6; doi:10.1007/978-1-59745-157-4_15)

· Results. Authors claim to have significant differences in several results that are not quantified and are not clear. They also do not explain why they treat lysosomes with just protease inhibitors and they do not add also lysosomal inhibitors such as NH4CL. They also do not really check the glycosylation status of LAMP2A despite having the tools to do so. In addition, all the brain sections shown are at different depths, so they are not comparable.

· Results, line 106. The explanation of the CMA photo-activable reporter is not correct.

· Results, line 112. Authors mention CMA substrates that are not addressed in the text.

· Results, line 117. The description of the results obtained in Fig 1c does not match what is observed in the figure. The expression of MEF2D and GAPDH seems to be altered with the different inhibitors.

· Results, line 294. Authors cannot state with only an Immunoprecipitation, what effects there may be on CMA activity.

Minor points:

· Results, line 413. There is a typo.

· Results, line 429. The text and the figures mentioned do not match.

· Results, line 466. Authors do not mention PDL-2 in the text even though it is included in supplementary figure 8a.

· Methods. The brain coordinates where the stereotactic procedure was performed should be indicated.

· Figure 5E. They show the images and quantification of tumor volume in mice with shC or shLAMP2A GSC 23, and how the

volume increases upon MTS4 upregulation. In the text, describing the results, they indicate that the knock down of LAMP2A in GSC23 (a GSC line with low MTS4 expression) had minimal effects on tumorigenicity of GSCs. However, in the figure, it is shown a clear reduction of the tumor in shLAMP2A with a significant statistical analysis.

· Supplementary Figure 3d. In order to verify the antibody T136A specificity, it should be tested in the single and double mutants generated for the study, not only in the 3A mutant.
· Figure 7 and supplementary figure 6. The cytotoxic effect of CD8 T cells should be confirmed with a double staining of CD8 and GZMB to confirm the colocalization. They could perform further analysis to confirm the functionality. In addition, authors could check the reduction of immunosuppressive T cell populations by IHC and by flow cytometry.

· Figure 11. An IHC analysis of GB patient samples is shown as well as a correlation analysis between the studied markers. In material and methods, authors describe that they have defined a score in order to perform the correlation analysis between the high and low expression of the markers. Nevertheless, the ranges the use for high and low expression are not well stablished. For instance, a sample with a score of 3 or 4 could be high and low at the same time according to their criteria. In addition, it is not mentioned in the text.

Version 1:

Reviewer comments:

Reviewer #1

(Remarks to the Author)
The authors have addressed my comments, except the code availability as per Nature communications' guidelines.

Reviewer #2

(Remarks to the Author)
We appreciate and applaud the authors' thoughtful and substantial revisions in response to our prior feedback. The manuscript is now suitable for publication, pending resolution of a few minor comments outlined below.

Minor Comments:

Clarification of CMA Marker Interpretation:
Page 6, Results, Line: 104-116:
The authors quite effectively demonstrate increased CMA activity in GSCs compared to non-GSCs with the PA-mCherry-KFERQ reporter. For clarity, however, it would be helpful to include a brief description of how puncta per cell reflects CMA activity and to differentiate this measurement from general lysosomal activity, given the centrality of this assay.

Expanded Discussion on CMA Regulation:
Page 9-10, Line: 180-194:
The authors well demonstrate MST4-LAMP2A interactions in conditions of stress (IR and starvation). Perhaps mention in brief the overall implications of this stress-induced interaction within the tumor microenvironment, such as how it may regulate GSC behavior in vivo under conditions of hypoxia or starvation commonly encountered within GBM tumors.

Lysosomal Protease Inhibition Consistency:

Page 8, Lines: 156-163 (Methods in Rebuttal response, Minor Comment 5):

Authors detailed in the rebuttal the explicit use of a protease inhibitor cocktail other than the LN (leupeptin/NH4Cl). However, a transitional mention in main manuscript methods or figure legends would raise transparency and methodological clarity in the light of the nuanced difference between LN and the more general PI cocktail.

Depth of Immunophenotyping in Syngeneic Models:

The authors have been able to address previous reviewer recommendations regarding the immunological mechanisms of CMA modulation. An inclusion of a short discussion sentence in the revised manuscript acknowledging the potential role of other significant immune cells beyond CD8+ T cells (Tregs, MDSCs, TAMs), although briefly, would provide a complete immunological perspective, especially since potential future research might venture into exploring these avenues.

Reviewer #4

(Remarks to the Author)
In the revised version, the new experiments added, provide evidence that TCS1/2 and TET3 are CMA substrates in human GSCs and could be used as therapeutic targets. However, there is not yet a clear link between the described mechanism and the inhibitor used. Additionally, several major points needs to be addressed so that the work meets the standards of the

journal.

• The authors state in the introduction that “the specific role of CMA in these cells [GSCs] is yet to be elucidated”, and in the first results section, they conclude that “these result//s indicated that CMA is required for GSC stemness and tumorigenicity”. However, these results are just a validation of the study already published in 2022 by Auzmendi-Iriarte et al. (doi.org/10.1158/0008-5472.CAN-21-2161). Although they could include these results as supplementary material to give context to the subsequent analysis of LAMP2A stability in the lysosomes of GSCs, the authors of this paper cannot include the first section of results as novel. In addition, they should elaborate further in the introduction and discussion on the work of Auzmendi-Iriarte et al. to expand the information. Overall, the authors should restructure the article in detail to actually report the mechanism they are describing.

• With the new experiments provided, the authors show that the inhibitor PPD does not affect the phosphorylation state of LAMP2A and that it inhibits its multimerization (Supplementary Fig. 8d-g). However, these results increase the lack of connection between the MST4-LAMP2A regulation and the use of PPD in the study. The results obtained with the inhibitor PPD both in vitro and in vivo are very promising, but do not justify why the authors have included this inhibitor in their therapeutical strategies when, apparently, it has no relevance on the described mechanism. It would be more appropriate for authors to submit the work to an autophagy journal, as without a specific inhibitor with effect on the in vivo models, the described regulatory mechanism lacks translational impact.

• In the response to reviewers’ comments, the authors state that they have not been able to perform the in vivo model with human GSC lines because “human GSCs are unable to engraft in immunocompetent C57BL/6 mice due to species-specific barriers”. However, they have also not tried the different therapeutic strategies in BALB/c nude mice that could perfectly well develop human GSCs tumors. In addition, there are other authors who have used human glioblastoma cells lines to develop a tumor in immunocompetent mice (Molina et al., 2022, doi.org/10.3389/fcell.2022.797945; Garcia et al., 2014, doi.org/10.1186/1471-2407-14-923). Therefore, without the in vivo experiments using human glioma cells the study lacks the translational impact necessary to get the standars of Nature Communications.

• Although the authors have followed the request to include papers on the physiological significance of CMA, they have not updated the introduction in accordance with the new works cited.

• Fig. 5A- Authors show some redundant analyses, previously published by Auzmendi-Iriarte et al., 2022 (doi.org/10.1158/0008-5472.CAN-21-2161), which are the original source of the RNAseq study used.

Li, Sheng and Li et al studied how chaperone-mediated autophagy (CMA) affects the tumor activity of glioblastoma (GBM). Using multiple lines of evidence, the authors identified MST4 as an interaction partner of LAMP2A, the only known lysosomal CMA receptor, and that its phosphorylation of LAMP2A enhanced LAMP2A's stability in the lysosome, CMA activity and GBM stem cell tumorigenicity. Next, using mouse models, the authors found that inhibiting CMA activity through knockdown of LAMP2A or MST4 led to reduced tumor growth and higher survival, which was mediated by T cell immune response. Mechanistically, the authors showed that CMA enhanced tumor activity via suppression of TSC1/2 proteins, which are negative regulators of the mTORC1 pathway, and via suppression of TET3 protein, which upregulates the cGAS-STING pathway via DNA demethylation. Finally, the authors showed the effectiveness of a GBM treatment strategy that combined CMA inhibition with radiotherapy and immune checkpoint therapy.

I am not qualified to comment on the biological novelty of the study. Besides that, the study is an impressive endeavor, as evidenced by the large amount of effort that has gone into it. I especially appreciate that the authors were able to verify their findings in GBM patients. At the editor's discretion, I think the study contains enough information for two separate papers.

Major comments:

1. The authors have not made their code available, especially for the RNA-seq analyses, for review.
2. Could the authors discuss how the GSC cell line 23 still shows higher activation of CMA compared to non-GSC cell lines (Fig 1), despite the former's very low expression of MST4 (Fig 5a)?
3. Did the authors use the same data for the red survival curve in Fig 7j and the black survival curve in Fig 10d? They look quite similar.
4. The authors should provide information on the characteristics of the 83 patients analyzed in Fig 11 (similar to the Table 1 in clinical papers). How did the authors take into account potential confounders when analyzing the clinical samples? Did the patients have any noteworthy co-morbidities?

Minor comments:

1. What statistical test did the authors use for the sphere-forming frequency analyses (those like Fig 1f). Why do those plots always have upside down triangles at y-values < -3 and x-values = 20 and 50?
2. Fig 1a, d: the error bars in the quantification of puncta per cell look unusually small compared to the variance of the data, and the error bars of different groups look almost identical to one another.
3. Is Fig 1c missing the results after treatment with NH4Cl? It was mentioned in the figure caption and the text (lines 114, 115).
4. Fig 1d: the left images show cell lines M83 and 23, while the right plot shows cell lines M83 and 456. Was this intentional?
5. Fig 2: did the author use LN as the protease inhibitor?
6. Fig 4b-d, g-h: the authors should also show the P-values comparing the blue and black data.
7. Fig 5c: please indicate the P-values on the legend like Fig 4d.
8. Fig 6a: the x-axis should say “0.00” instead of “-0.00”.
9. Fig 7j: the authors should show the P-value comparing the green and blue lines.
10. Lines 549 and 554: did the authors mean GSCs instead of “CSCs”?
11. Line 720: “quired” typo.

**Manuscript Number: NCOMMS-25-06239-T-R1**

**Point-to-Point Responses to Reviewer's Comments**

We appreciate the enthusiasm with which the editor and the four reviewers received our initial submission. We have addressed all of their concerns/questions in the revised manuscript and have included substantial new results in this revised submission. We believe that the revised manuscript provides a more thorough and informative presentation or our research, and we are grateful to the reviewers for their suggestions. Thus, we are pleased to submit the revised version of this manuscript for further consideration. Below are point-by-point responses to the comments:

***Reviewer #1:***

*Li, Sheng and Li et al studied how chaperone-mediated autophagy (CMA) affects the tumor activity of glioblastoma (GBM). Using multiple lines of evidence, the authors identified MST4 as an interaction partner of LAMP2A, the only known lysosomal CMA receptor, and that its phosphorylation of LAMP2A enhanced LAMP2A's stability in the lysosome, CMA activity and GBM stem cell tumorigenicity. Next, using mouse models, the authors found that inhibiting CMA activity through knockdown of LAMP2A or MST4 led to reduced tumor growth and higher survival, which was mediated by T cell immune response. Mechanistically, the authors showed that CMA enhanced tumor activity via suppression of TSC1/2 proteins, which are negative regulators of the mTORC1 pathway, and via suppression of TET3 protein, which upregulates the cGAS-STING pathway via DNA demethylation. Finally, the authors showed the effectiveness of a GBM treatment strategy that combined CMA inhibition with radiotherapy and immune checkpoint therapy.*

*I am not qualified to comment on the biological novelty of the study. Besides that, the study is an impressive endeavor, as evidenced by the large amount of effort that has gone into it. I especially appreciate that the authors were able to verify their findings in GBM patients. At the editor's discretion, I think the study contains enough information for two separate papers.*

**Response:** We greatly appreciate the reviewer's positive comments and excellent recommendations for improving the manuscript. We have followed up on each of the concerns, indicated by reviewer #1, by performing all suggested experiments. We have included new results in revised figures with accompanying text descriptions.

*1. The authors have not made their code available, especially for the RNA-seq analyses, for review.*

**Response:** We sincerely apologize for the oversight in clarifying data accessibility. To address this, we have deposited the mass spectrometry dataset identifying LAMP2A-interacting kinases (including MST4), along with peptide counts and coverage, in the PRIDE repository under accession number [PXD060464]. The RNA-seq analysis utilized publicly available data from GSE181556. Proteomic comparisons were derived from dataset PXD027069. Both datasets originate from a prior study by Auzmendi-Iriarte et al. *(Cancer Res*. 2022, 82(7):1283–1297.). This information has been explicitly stated in the revised manuscript (page 9, line 180; page 17, line 354; and page 41, line 883 and 889) to ensure transparency.

We regret any confusion caused and appreciate the opportunity to clarify these critical details.

*2. Could the authors discuss how the GSC cell line 23 still shows higher activation of CMA compared to non-GSC cell lines (Fig 1), despite the former's very low expression of MST4 (Fig 5a)?*

**Response:**

This is an excellent question. To address why GSC 23 cells exhibit higher CMA activation compared to non-GSC cell lines despite their very low MST4 expression, we conducted a detailed analysis of LAMP2A, the key receptor for CMA.

Firstly, we measured total and lysosomal LAMP2A levels in various GSC and non-GSC lines. The mRNA levels of *LAMP2A* were similar between GSC 23 and non-GSCs, but GSC 23 exhibited lysosomal LAMP2A protein levels comparable to other GSC lines and significantly higher than non-GSCs (PBP Fig.1 a, b). These results suggest that the increased CMA activity in GSC 23 may be linked to higher lysosomal LAMP2A levels.

Secondly, we assessed the phosphorylation status of LAMP2A, as phosphorylation is crucial for regulating lysosomal LAMP2A protein levels. When comparing GSC 23 cells (with low MST4) to M83 cells (with normal MST4) and non-GSC cell lines (U251 and LN229), we found that GSC 23 cells had higher LAMP2A phosphorylation levels (PBP Fig.1 c), not at the T136 site, implying that MST4-independent signaling pathways may be involved.

Recently, it has been reported that lysosomal p38 MAPK directly phosphorylates LAMP2A at T211 and T213, leading to its membrane accumulation (Li W, *et al.*, *Nat Commun*. 2017;8(1):1763.). To test whether p38α MAPK plays a role in maintaining lysosomal LAMP2A levels and CMA activity in GSC 23 cells, we treated them with SB203580, a pharmacological inhibitor of p38α MAPK. The finding revealed that treatment with SB203580 resulted in diminished levels of phosphorylated LAMP2A and lysosomal LAMP2A, as well as a reduction in the association of MEF2D—a recognized CMA substrate—with lysosomes, thereby leading to an increased accumulation of MEF2D in the total cell lysate (PBP Fig.1 d). These results suggest that the phosphorylation of LAMP2A by p38α MAPK is critical for the maintenance of basal CMA activity in GSC 23 cells.

The data supporting these conclusions are included in the revised Supplementary Fig. 1c-d, Supplementary Fig. 4f-g, and described in detail on page 7, line 131-135 and page 16, line 336-343 of the revised manuscript.

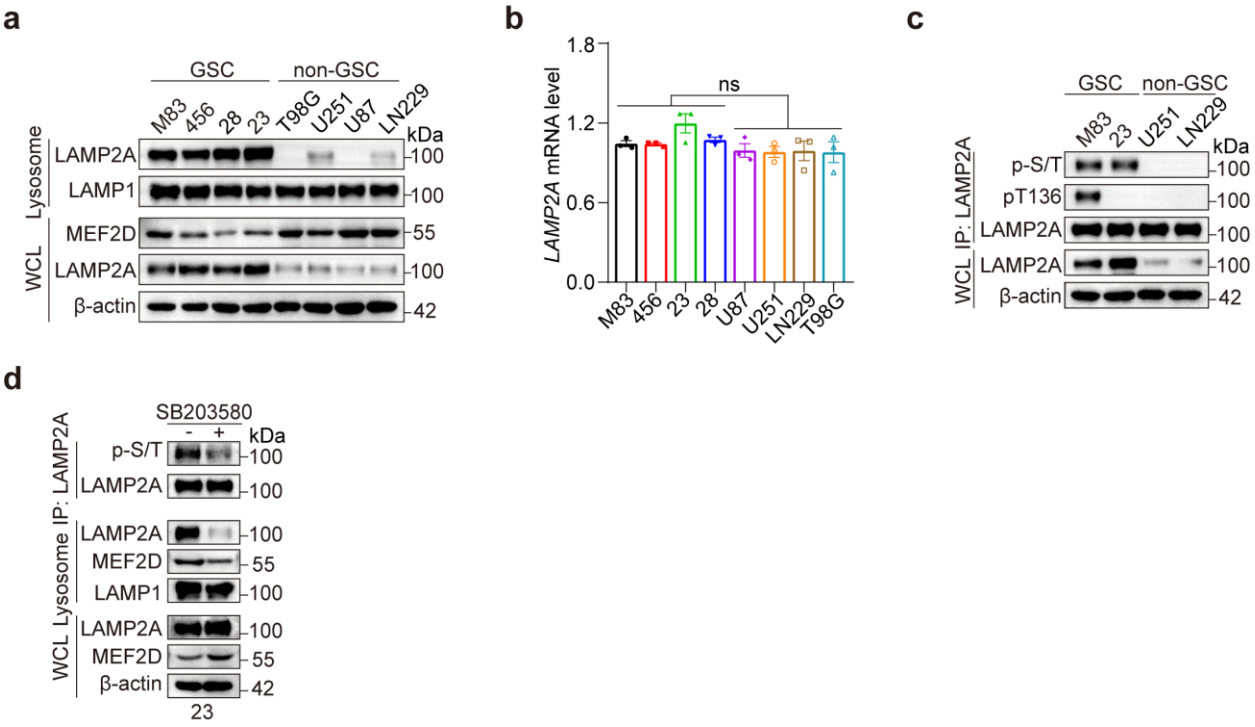


**PBP Fig. 1 a:** IB analyses for LAMP2A and MEF2D, CMA targets, in whole-cell lysates (WCL) and lysosomal fractions of GSCs and non-GSCs. β-actin and LAMP1 were used as loading controls for WCL and lysosomal samples, respectively.

**PBP Fig. 1 b:** Quantitative real-time PCR (qPCR) assessment of mRNA level of *LAMP2A* in GSCs and non-GSCs. Data are presented as the mean ± S.E.M. n = 3 independent experiments. ns, not significant by one-way ANOVA with Tukey's multiple comparisons test.

**PBP Fig. 1 c:** IP-IB analyses for indicated proteins in WCL of GSCs (M83 and 23) and non-GSCs (U251 and LN229).

**PBP Fig. 1 d:** IP-IB analyses for indicated proteins in WCL and lysosomal fractions of GSC 23 with or without p38 MAPK inhibitor SB203580 (10 μM) treatment for 12 hours.

*3. Did the authors use the same data for the red survival curve in Fig 7j and the black survival curve in Fig 10d? They look quite similar.*

**Response:** We sincerely appreciate the reviewer's careful observation regarding the similarity between the survival curves in Fig. 7j and Fig. 10d. Through meticulous re-examination of our experimental records and raw data, we identified an inadvertent data processing error in GraphPad Prism where the survival data for the C57BL/6 mice with intracranial GL261-sh-Lamp2a/Ctrl tumors (black curve in Fig. 10d) was incorrectly applied to the CT-2A-sh-Lamp2a tumor group (red curve in Fig. 7j). This occurred during data entry when we mistakenly misclassified the mouse groups, despite the fact that these two groups involved different host cells while sharing the same treatment/genetic modification.

To comprehensively address this issue and ensure data integrity, we have implemented the following corrective measures:

1) We have replaced the erroneous data in Fig. 7j (now renumbered as Fig. 6n) with the correct CT-2A-sh-Lamp2a tumor survival data (original cohort: n = 5; survival endpoints: 25, 31, 34, 40, 43 days; median 34 days). To enhance statistical reliability, we expanded the sample size by including 3 additional mice (new endpoints: 28, 30, 32 days), resulting in a combined median survival of 31.5 days (n = 8). This expansion preserved the original survival differences between experimental groups.
2) We conducted a completely new validation experiment with the CT-2A-sh-Lamp2a group (n = 5), which yielded consistent results (endpoints: 25, 26, 29, 37, 40 days; median 29 days; $p$ = 0.61 by log-rank test compared to the original data). These validation data are now presented in revised Fig. 9d.
3) The original data in Fig. 10d (endpoints: 25, 31, 34, 40, 43 days; median 34 days) have been retained in the updated Supplementary Fig. 9g.

We deeply regret this oversight and have implemented additional data verification steps to prevent similar errors in future work. Importantly, our new experimental results robustly confirm the reproducibility of our initial findings. We are particularly grateful to the reviewer for bringing this to our attention, as it has significantly improved the manuscript's accuracy and reliability.

*4. The authors should provide information on the characteristics of the 83 patients analyzed in Fig 11 (similar to the Table 1 in clinical papers). How did the authors take into account potential confounders when analyzing the clinical samples? Did the patients have any noteworthy co-morbidities?*

**Response:** We sincerely appreciate the reviewer's insightful suggestions regarding patient characteristics and statistical methodology. Below are our point-by-point responses with corresponding revisions:

1) As suggested, we have now provided comprehensive demographic and clinical data in the newly added Supplementary Table 2, which includes: Demographics: age distribution (mean ± SD: 49.6 ± 13.4 years) and sex ratio (46 male, 37 female); Tumor stratification: WHO grade (IV: 41, III: 13, II: 19, I: 4) with histological verification; Comorbidity profiles: cephalalgia (n = 20), epilepsy (n = 3), seizure (n = 5), dizziness (n = 3), and other conditions (n = 14).
2) To mitigate potential confounding effects, we implemented block randomization to ensure balanced distribution of age/sex across experimental cohorts, and adopted blinded analysis protocol where laboratory measurements (MST4, LAMP2A pT136, etc.) were conducted independently of clinical data. Our analysis concentrated exclusively on the expression levels of the target proteins in patient specimens, thereby minimizing the influence of other confounding variables on our findings.
3) We systematically documented comorbid conditions in Supplementary Table 2, which includes: cephalalgia (n = 20, 24.1%), epilepsy (n = 3, 3.6%), seizure (n = 5, 6.0%), dizziness (n = 3, 3.6%) and others (n = 14, 16.9%); however, these comorbidities were excluded from primary survival analyses to avoid confounding effects, consistent with RECORD guidelines for neuro-oncological studies.

We have incorporated the above updates into the Supplementary Table 2 and Methods section of the revised manuscript (IHC analysis of clinical glioma specimens on page 53-54, line 1135-1143).

*Minor comments:*

1. *What statistical test did the authors use for the sphere-forming frequency analyses (those like Fig 1f). Why do those plots always have upside down triangles at y-values < -3 and x-values = 20 and 50?*

**Response**: Thank you for your questions. Regarding the sphere-forming frequency analyses (as depicted in Fig 1f), The sphere-forming frequency was calculated using the Extreme Limiting Dilution Analysis (ELDA) platform (Hu & Smyth, *J. Immunol*. Methods, 2009). ELDA applies a likelihood ratio test (not t-tests) to compare the frequency of sphere-initiating cells between groups. This method is optimized for small sample sizes and provides higher statistical power than traditional approaches.

Regarding the inverted triangles in plots ($y < -3$, $x = 20, 50$), the inverted triangles (▼) are automatically generated by the ELDA software to indicate data points beyond the default y-axis range (here, $y < -3$). For example: When the log (fraction of without sphere) drops below -3, ELDA truncates the y-axis and marks these points with ▼. At high cell densities ($x = 20, 50$), some groups (e.g., sh-C+Vec) showed near-complete sphere formation (0 wells without sphere), resulting in $\log(0) = -\infty$. ELDA substitutes these values with a predefined lower bound ($y = -3$) and uses ▼ to denote censored data.

2. *Fig 1a, d: the error bars in the quantification of puncta per cell look unusually small compared to the variance of the data, and the error bars of different groups look almost identical to one another.*

**Response**: We appreciate the reviewer's critical observation. In Fig. 1a and 1d, the quantitative data (fluorescent puncta/cell) are presented as mean ± S.E.M. (standard error of the mean) with individual data points overlaid. The S.E.M. values appear small because they were calculated from a large sample size (n = 40 cells per group, derived from 3 independent biological replicates). S.E.M. decreases with increasing sample number, reflecting the precision of the mean estimate rather than the raw data variability.

The similar S.E.M. magnitudes across groups resulted from comparable sample sizes and variance homogeneity, which was confirmed by Levene's test ($p > 0.05$) prior to one-way ANOVA. Statistical significance ($p < 0.05$) was determined by ANOVA followed by Tukey's post-hoc test.

3. *Is Fig 1c missing the results after treatment with NH4Cl? It was mentioned in the figure caption and the text (lines 114, 115).*

**Response**: We sincerely appreciate the reviewer's careful observation regarding the presentation of $NH_4Cl$ results in Fig. 1c. To clarify, the "LN" label in this figure represents the combined treatment of leupeptin (10 μM) and ammonium chloride ($NH_4Cl$, 20 mM), which were co-administered as a dual-inhibitor approach to comprehensively block lysosomal degradation (leupeptin as a protease inhibitor and $NH_4Cl$ as a lysosomal acidification blocker). Recognizing that the original labeling might have caused confusion, we have amended the text from "leupeptin and ammonium chloride (LN)" to "leupeptin and ammonium chloride ($NH_4Cl$), LN" and have updated the figure legend to explicitly define: "LN (10 μM leupeptin and 20 mM $NH_4Cl$)" This modification enhances clarity and is consistent with the methodology outlined in the text. We regret any confusion stemming from the initial presentation and thank you for allowing us to clarify this important aspect.

The updated manuscript now includes these revisions in page 6, line 114-115 and the figure legend (page 63, line 1466-1469).

4. *Fig 1d: the left images show cell lines M83 and 23, while the right plot shows cell lines M83 and 456. Was this intentional?*

**Response**: We sincerely thank the reviewer for identifying this labeling discrepancy in Fig. 1d. Upon re-examining the figure, we confirm that the left panel incorrectly labeled cell line 456 as 23 during image assembly. This was an unintentional error in figure preparation. The labels in the left panel of Fig. 1d have been revised to accurately reflect M83 and 456 cell line.

5. *Fig 2: did the author use LN as the protease inhibitor?*

**Response**: We sincerely appreciate the reviewer's insightful question regarding the protease inhibitors used in Fig. 2. To clarify, we did not employ the LN combination (leupeptin + $NH_4Cl$) in these experiments. Instead, we utilized a comprehensive protease inhibitor (PI) cocktail consisting of: 10 μM leupeptin (targeting serine/cysteine proteases), 10 μM AEBSF (serine protease inhibitor), 1 μM pepstatin A (aspartic protease inhibitor), and 100 μM EDTA (metalloprotease inhibitor). This optimized cocktail was applied to freshly isolated intact lysosomes for 10 minutes at 0°C to achieve broad-spectrum protease inhibition and to prevent LAMP2A luminal degradation. Our approach follows well-established methodologies for lysosomal studies, as documented by Kaushik and Cuervo (*Methods Enzymol.* 2009, 452:297-324.).

We have revised the method for analyzing the degradation rate of LAMP2A in isolated lysosomes in the Immunoblot (IB) analysis section, on page 45, line 958-964.

6. *Fig 4b-d, g-h: the authors should also show the P-values comparing the blue and black data.*

**Response**: Thank you for your suggestion. We have included the *P*-values comparing the blue and black data in revised Fig. 4b-d, g-h.

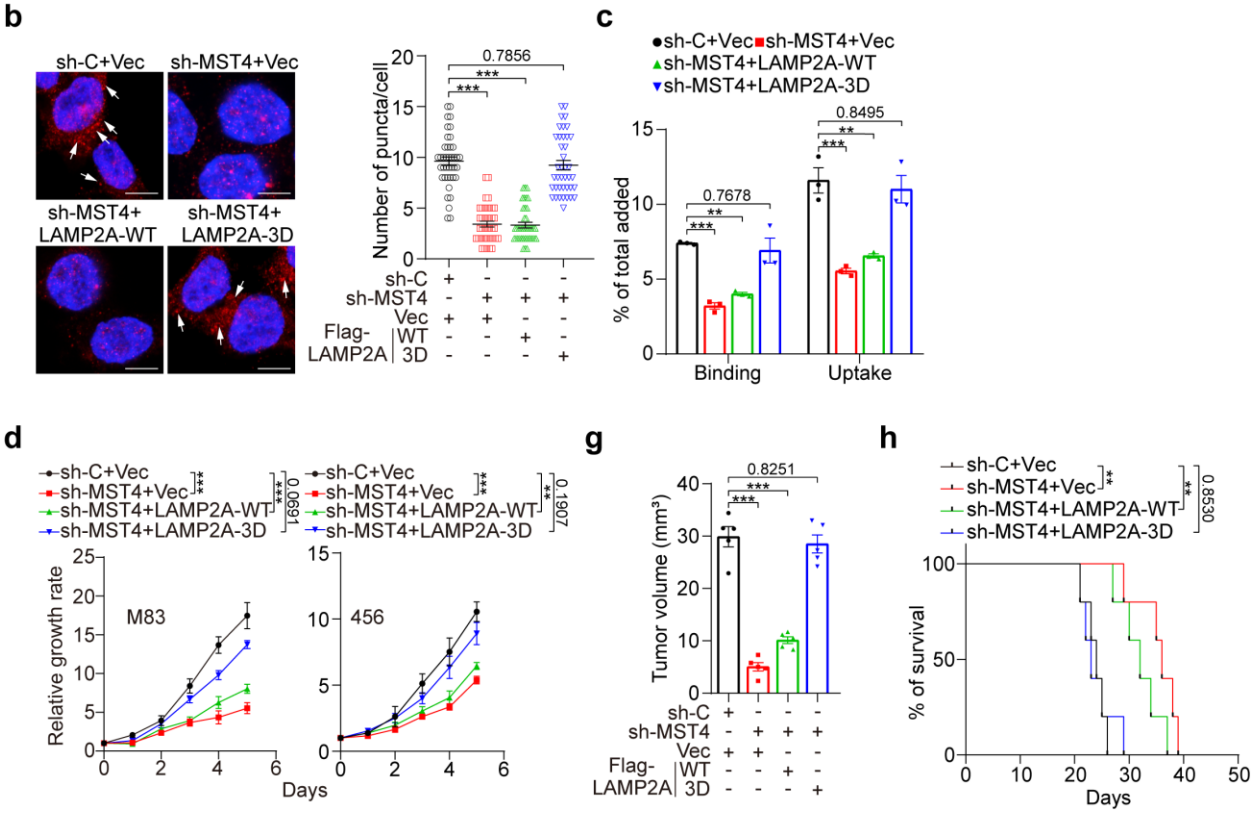


**PBP Fig. 2 b:** Representative images (left) and quantification (right) of CMA activity detection by KFERQ puncta numbers in GSC M83 cells with indicated modifications. Data are presented as the means ± S.E.M. n = 40 randomly selected cells. Scale bar, 10 μm.

**PBP Fig. 2 c:** *In vitro* binding and uptake assay of GAPDH by the lysosome in GSC M83 cells with indicated modifications. Data are presented as the means ± S.E.M. n = 3 independent experiments.

**PBP Fig. 2 d:** Cell proliferation of GSC M83 and 456 cells with indicated modifications. Data are presented as the means ± S.E.M. n = 3 independent experiments.

**PBP Fig. 2 g:** Quantitative analysis of tumor volume from athymic (BALB/c Nude) mice intracranially implanted with GSC M83 cells with indicated modifications. Data are presented as the means ± S.E.M. n = 5.

**PBP Fig. 2 h:** Kaplan-Meier survival curves of athymic (BALB/c Nude) mice intracranially transplanted with GSC M83 cells with indicated modifications. n = 5/group.

Statistical significance was assessed using one-way ANOVA with Dunnett's multiple comparisons test (**b**, **c**, **d**, **g**) or log-rank test (**h**). $^{**}p < 0.01$, $^{***}p < 0.001$.

*7. Fig 5c: please indicate the P-values on the legend like Fig 4d.*

**Response**: We sincerely appreciate the reviewer's attention to detail and constructive feedback. In response to your suggestion: The exact *P*-values for all statistical comparisons in Fig. 5c (now

updated to Fig. 4m) have now been added to the figure legend, mirroring the format used in Fig. 4d.

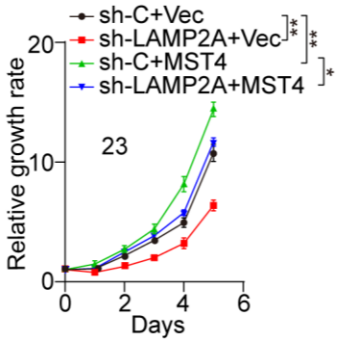


**PBP Fig. 3:** Cell proliferation of GSC 23 cells with indicated modifications. Data are presented as the means ± S.E.M. n = 3 independent experiments. *$p$ < 0.05, **$p$ < 0.01 by one-way ANOVA with Tukey's multiple comparisons test.

8. *Fig 6a: the x-axis should say "0.00" instead of "-0.00".*

**Response:** Thank you for pointing out this error. The negative sign in "-0.00" on the x-axis of Fig. 6a (now updated to Fig. 5a) was inadvertently retained during data formatting. We have corrected it to "0.00" in the revised manuscript to accurately reflect the scale. We apologize for any confusion this may have caused.

9. *Fig 7j: the authors should show the P-value comparing the green and blue lines.*

**Response:** We appreciate the reviewer's suggestion. In the revised Fig. 7j (now updated to Fig. 6n), we have now included the *P*-value for the comparison between the green and blue line ($p$ = 0.0319), following the same statistical annotation style as in other figures. This addition enhances the completeness of the statistical analysis presented.

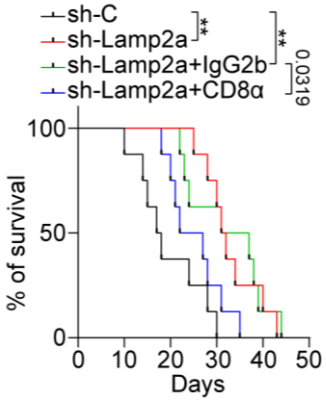

**PBP Fig.4:** Kaplan-Meier survival curves of C57BL/6 mice intracranially transplanted with CT-2A cells with indicated modifications and treatments. n = 8/group. Statistical significance was assessed using log-rank test. $^{**}p < 0.01$.

*10. Lines 549 and 554: did the authors mean GSCs instead of "CSCs"?*

**Response:** We sincerely appreciate the reviewer's careful attention to our terminology usage. Upon reviewing line 549 and 554, we confirm that "CSCs" was indeed intended to refer generally to "cancer stem cells" rather than specifically to "glioma stem cells (GSCs)." We acknowledge that this created potential confusion since we had not explicitly defined the CSC abbreviation earlier in the manuscript. To prevent any misunderstanding, we have now revised both instances to spell out "cancer stem cells" in full. We apologize for this oversight and are grateful to the reviewer for identifying this point of ambiguity. These modifications have been updated on page 32, line 678 and 683 of the revised manuscript.

*11. Line 720: "quired" typo.*

**Response:** We sincerely apologize for this oversight. The typo "quired" in line 720 has been corrected to "obtained" in the revised manuscript (page 41, line 883). We have also conducted an additional spell-check of the entire text to prevent similar errors.

***Reviewer #2:***

*This study by Li et al. explores the role of the MST4-LAMP2A axis in regulating chaperone-mediated autophagy (CMA) and its impact on glioblastoma stem cell (GSC) proliferation. The authors report elevated levels of LAMP2A in patient-derived GSCs and demonstrate that LAMP2A downregulation in glioma cell lines reduces GSC proliferation in vitro while improving survival in orthotopic immunodeficient mouse models. Mechanistically, they identify MST4 as a key regulator that phosphorylates LAMP2A, enhancing its stability in GSC lysosomes and promoting mTORC1 activation through the degradation of its negative regulators, TSC1 and TSC2. Therapeutically, the study links this pathway to immune evasion via suppression of the cGAS-STING axis and shows that inhibiting CMA synergizes with anti-PD-1 therapy in a GL261 syngeneic model. Overall, the paper provides a comprehensive mechanism for CMA regulation and presents a strong case for targeting CMA as a potential therapeutic strategy for glioblastoma.*

**Response:** We thank the reviewer for the enthusiasm and the positive comments. We also appreciate the reviewer's excellent comments and suggestions. We have performed additional experiments to address the reviewer's concerns.

*Major points:*

*1-The paper is very comprehensive with the introduction explaining the key players of the mechanism behind CMA modulation for GSCs. The results flow well with logical progression of the rationale behind targeting MST4 or LAMP2A*

**Response:** We appreciate the reviewer's positive feedback on the manuscript's logical structure and thorough introduction. We have preserved this level of rigor in the revised version to ensure clarity and coherence throughout the study.

*2-Given recent studies that have highlighted the importance of efferocytosis in the tumor microenvironment with autophagy, the authors should mention this process as it is directly impacted by their proposed therapy. This would also strengthen the study's scope of mechanism in that it would functionally incorporate myeloid cells into the pathways described*

**Response:** We sincerely appreciate the reviewer's valuable suggestion concerning the significant role of efferocytosis in shaping the immunosuppressive tumor microenvironment (TME) through autophagy-dependent mechanisms. Our findings indicate that chaperone-mediated autophagy (CMA) regulates the cGAS/STING pathway by facilitating lysosomal degradation of TET3. Recent study shows that LC3-associated phagocytosis (LAP) - an autophagy-related process - regulates efferocytosis-mediated immune suppression in TAMs by inhibiting STING signaling (Cunha LD, et al. *Cell*. 2018;175(2):429-441.). Considering the critical involvement of autophagy in efferocytosis—the process responsible for clearing apoptotic cells generated by DNA-damaging therapies such as radiotherapy—it would be worthwhile to further investigate whether CMA influences both the cGAS/STING signaling pathway and the anti-tumoral immune response via efferocytosis in myeloid cells. The potential interplay between CMA and efferocytosis presents novel therapeutic opportunities for targeting the immunosuppressive TME in glioblastoma (GBM).

We have included this discussion in the revised manuscript on page 34-35, line 728-747.

*3-GL261 is a very immunogenic model that is now out of favor compared to more resistant lines such as CT-2A and SB28. The preclinical orthotopic data could be strengthened by showing survival studies with these additional models*

**Response:** Thank you for your valuable suggestion. We have performed the additional survival studies with CT-2A preclinical orthotopic model. In this model, neither radiation monotherapy (IR) nor anti-PD-1 (αPD-1) checkpoint blockade demonstrated significant tumor suppression or survival benefit compared to control group (median survival: control 18 days vs IR 24 days, $p$ = 0.42; control 18 days vs αPD-1 22 days, $p$ = 0.26; PBP Fig.5 a-c). Notably, only the combination therapy exhibited significant tumor growth inhibition and survival prolongation (median survival: control 18 days vs αPD-1+IR 28 days, $p < 0.05$, PBP Fig.5 a-c). Importantly, reducing CMA components by Mst4 or Lamp2a knockdown significantly enhanced the effectiveness of both IR or αPD-1 monotherapy (median survival: sh-Lamp2a 29 days vs sh-Lamp2a+αPD-1 43 days or sh-Lamp2a+IR 45 days, $p < 0.05$; sh-Mst4 30 days vs sh-Mst4+αPD-1 42 days or sh-Mst4+IR 45 days, $p < 0.05$; PBP Fig.5 a-b, d-e). The most pronounced survival benefit was achieved through triple combination therapy incorporating CMA inhibition with IR and αPD-1 (median survival of 52 or 55 days versus 18 days in control, $p < 0.01$; PBP Fig.5 a-e).

Similar to the GL261 intracranial GBM model, we assessed the impact of the CMA inhibitor Polyphyllin D (PPD) on IR therapy and αPD-1 monoclonal antibody treatment in the CT-2A C57BL/6 intracranial GBM model. None of the individual treatments (IR, αPD-1, or PPD) demonstrated significant efficacy against CT-2A tumors (median survival: control 18 days vs IR 24 days, $p$ = 0.37; control 18 days vs anti-PD-1 23 days, $p$ = 0.35; control 18 days vs PPD 25 days, $p$ = 0.25; PBP Fig.5 f-h). Pairing the two therapies resulted in significantly survival benefits (median survival: 28, 29 or 31 days respectively, $p < 0.05$; PBP Fig.5 f-h). Most remarkably, the triple combination therapy (PPD+αPD-1+IR) produced the most potent anti-tumor effects, achieving a median survival of 42 days ($p < 0.01$ versus control; PBP Fig.5 f-h). These findings from both GBM models (GL261 and CT-2A) further supported our conclusion that inhibiting CMA creates an important therapeutic opportunity for immune checkpoint therapy in GBM.

These data have been incorporated into the revised Fig. 9a-h, with detailed descriptions provided on page 28-29, line 587-609 of the revised manuscript.

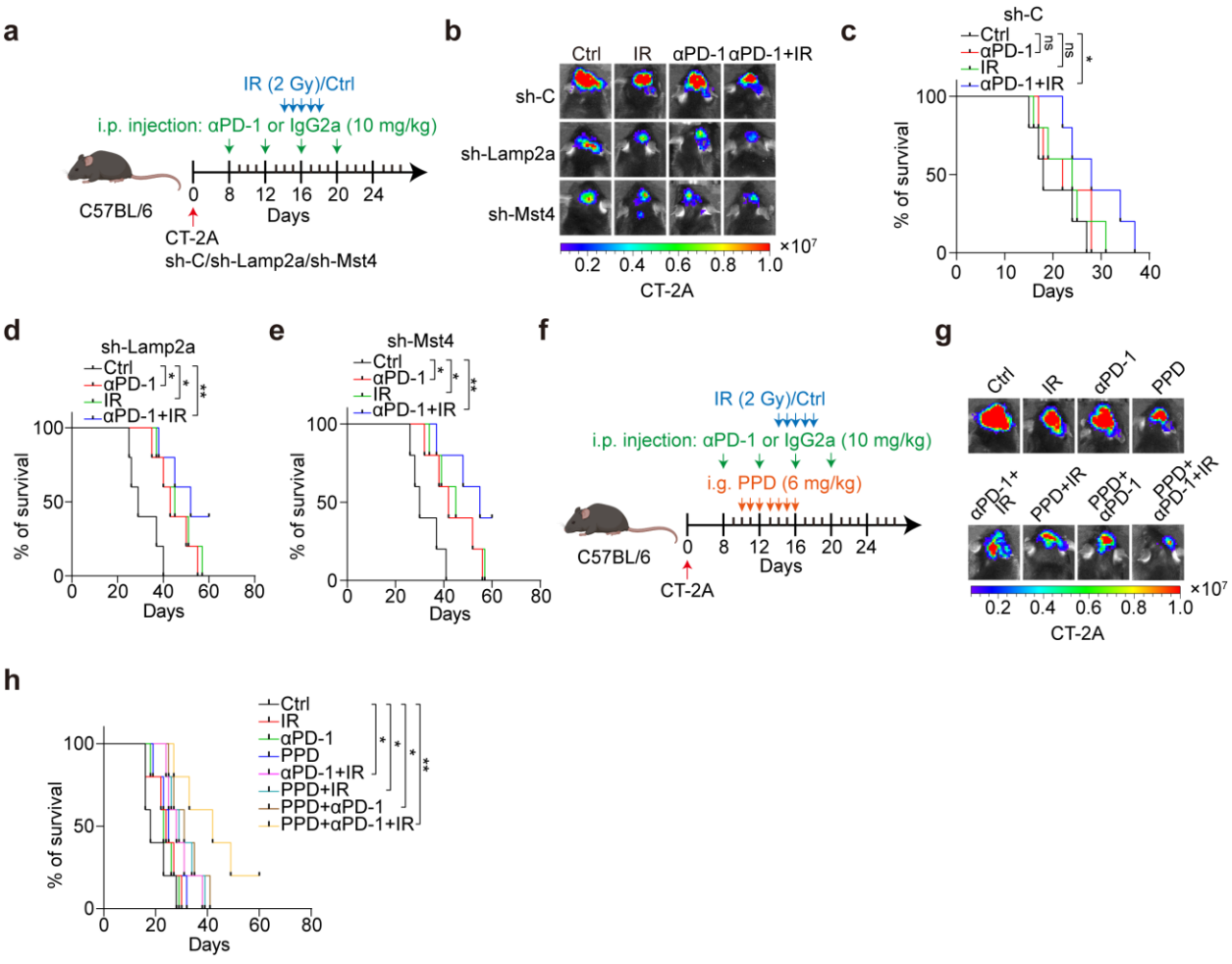


**PBP Fig. 5 a, f:** Scheme representing the experimental procedure.

**PBP Fig. 5 b:** Representative luciferase-based bioluminescence images of C57BL/6 mice with intracranially transplanted CT-2A cells with indicated modifications and treatments. Colored scale bars represent photons/s/cm$^2$/steradian.

**PBP Fig. 5 c-e:** Kaplan-Meier survival curves of C57BL/6 mice with intracranially transplanted with CT-2A cells with modifications and treatments. n = 5/group.

**PBP Fig. 5 g:** Representative luciferase-based bioluminescence images of C57BL/6 mice with intracranially transplanted CT-2A cells with indicated treatments. Colored scale bars represent photons/s/cm$^2$/steradian.

**PBP Fig. 5 h:** Kaplan-Meier survival curves of C57BL/6 mice with intracranially transplanted with CT-2A cells with indicated treatments. n = 5/group.

Statistical significance was assessed using log-rank test. ns, not significant. *$p$ < 0.05, **$p$ < 0.01.

*4-This study could be significantly strengthened by including further immunophenotyping beyond CD8+ T cells (e.g. Tregs, TAMs, MDSCs). By characterizing the immune microenvironment further (in both human tissue samples as well as in the syngeneic model), the role of CMA in impacting the immune milieu could be better understood. This would especially be helpful for expanding on the overlap with cGAS-STING and this strategy synergizing with anti-PD-1 as shown in the study.*

**Response:** We sincerely appreciate the reviewer's insightful suggestion regarding comprehensive immunophenotyping analysis, which has significantly strengthened our understanding of CMA's immunomodulatory effects in both human and murine systems.

To investigate the role of CMA in impacting the immune milieu in human GBM tissue samples, we adopted the CMA score, as described previously (Bourdenx, M. et al. *Cell*, 2021.184: 2696–2714.), by giving each gene expression value a weight (depending on their relevance on CMA) and directionality (as activator or inhibitor of CMA). Through analysis of human GBM samples from TCGA dataset, we found that CMA score was negatively correlated with CD8$^+$ T cells, while showing positive associations with immunosuppressive cell populations including TAMs and MDSCs. A non-significant trend was observed with regulatory T cells (Tregs) ($p$ = 0.323) (PBP Fig. 6a-f). These results suggest CMA's potential role in shaping an immunosuppressive tumor microenvironment.

Using the CT-2A syngeneic model, we further demonstrated that Mst4 knockdown reduced infiltration of immunosuppressive cells (Tregs, TAMs, and MDSCs; PBP Fig. 6g-i). Conversely, the reintroduction of LAMP2A-WT or -3D markedly reinstated the infiltration of these immunosuppressive cell populations (PBP Fig. 6g-i). These findings collectively highlight CMA's selective role in immune microenvironment modulation and provide mechanistic insights into its potential synergy with immunotherapies.

These findings are presented in the revised Fig. 6a and Supplementary Fig. 6a-e, n-p, and described in detail on page 21-22, line 431-439 and line 464-467). The newly developed experimental protocol has been incorporated into the Methods section (Bioinformatics analysis of immune infiltration based on CMA score on page 42-43, line 901-917, and Flow cytometric analysis on page 47-48, line 1002-1015).

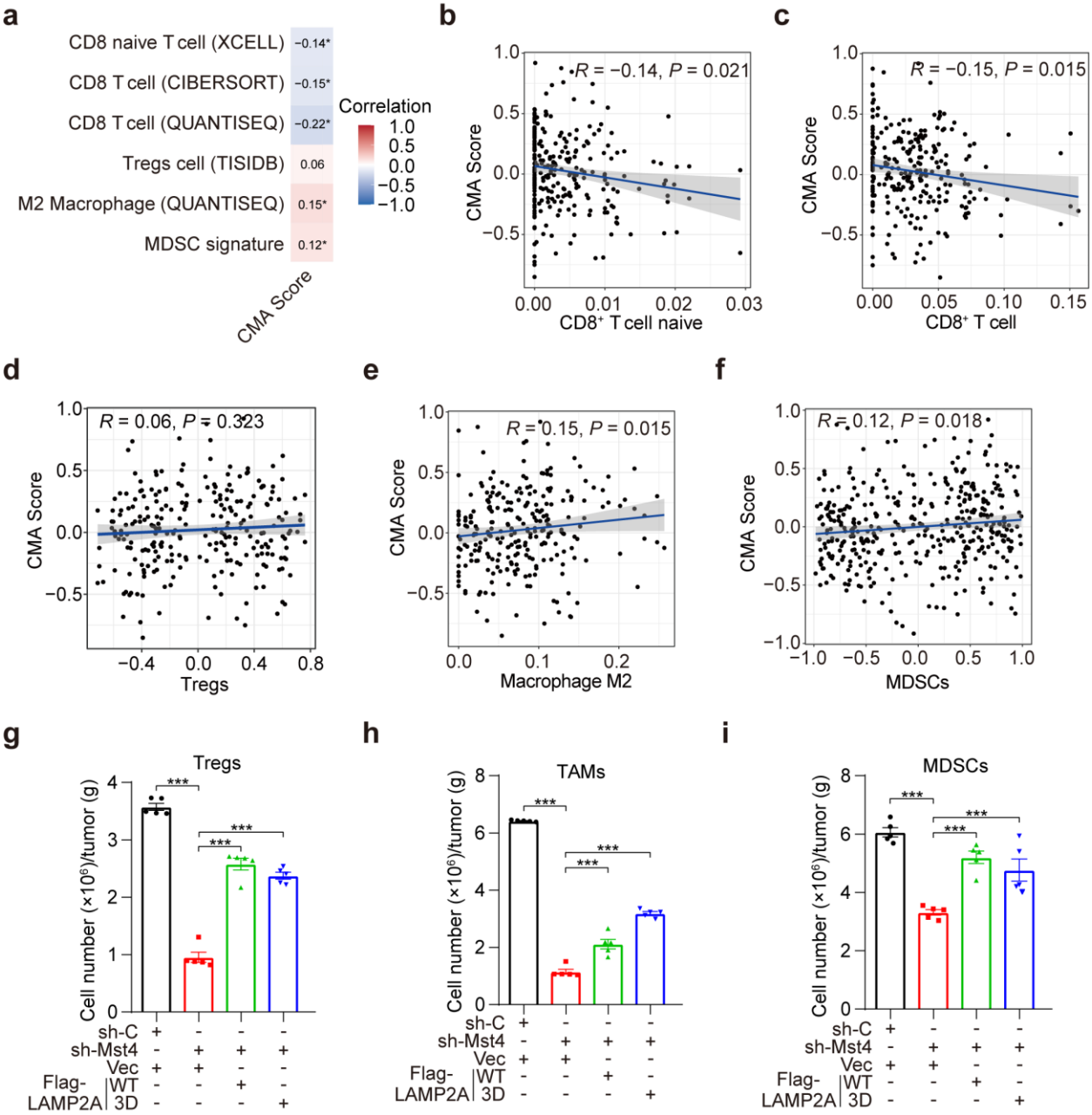


**PBP Fig. 6 a:** Spearman correlation heatmap between CMA activity scores and immune infiltration levels in TCGA-GBM dataset. Color gradient represents correlation coefficients, with numerical values and statistical significance (*p*-values) annotated.

**PBP Fig. 6 b-f:** Correlation analysis between CMA activity scores and immune cell infiltration profiles in TCGA GBM samples using TIMER2 or TISIDB databases.

**PBP Fig. 6 g-i:** Flow cytometric analyses of population of infiltrating Tregs (**g**), TAMs (**h**) and MDSCs (**i**) in tumor tissues from C57/BL6 mice with intracranial CT-2A cells transplants with indicated modifications. Data are presented as the means ± S.E.M. n = 5 independent experiments.

Statistical significance was assessed using one-way ANOVA with Tukey's multiple comparisons test. ***$p < 0.001$.

*Minor points:*

*-Please undergo mechanical revision for minor errors (i.e. line 51 Prior study has identified…)*

**Response:** We apologize for these oversights. The sentence in line 51 (now updated to line 49 in page 3) has been revised to " A prior study has identified…" to correct subject-verb agreement. A full grammar and syntax check have been performed across the manuscript, and all identified errors have been addressed.

***Reviewer #3:***

*In this study, Li et al show that CMA is upregulated in patient-derived glioblastoma stem cells characterized by a notable increase in the levels of the CMA receptor, lysosome-associated membrane protein type 2A (LAMP2A). Moreover, their experiments delineate an MST4-LAMP2A signaling pathway that modulates CMA activity and facilitates tumor initiation and immune escape of GSCs.*

*The results describing that CMA and LAMP2A are increased in patient-derived glioblastoma stem cells and associated with poor patient survival have been previously described (Auzmendi-iriarte et al Cancer Research). Similarly, that study described that CMA activity promotes tumor initiation and progression and revealed immune escape and metabolism as critical processes involved on them. Indeed, the OMIC data used in the study of Li et al were generated on the Auzmendi-iriarte study. Although the study of Li et al went deeper in the description of the molecular mechanisms underlying CMA activity, it does not present enough novelty and relevance to be published in Nature Communications. I I think the manuscript suits better in a specific journal of autophagy.*

**Response:** Thank you for your thorough evaluation of our manuscript and for raising concerns about its novelty and suitability for *Nature Communications*. We appreciate the opportunity to clarify the unique contributions of our study, which significantly extend beyond prior findings (e.g., Auzmendi-iriarte et al., *Cancer Research* 2022) and provide mechanistic and therapeutic insights with broad implications. Below, we address your points in detail and clarify the unique contributions, innovative insights, and scientific significance of our study that justify its publication in *Nature Communications*.

1. **Discovery of the MST4-LAMP2A signaling pathway.**

   While Auzmendi-iriarte et al. (*Cancer Research*, 2022) previously reported the upregulation of CMA and LAMP2A in glioblastoma stem cells (GSCs) and their association with poor patient prognosis, our work advances this field by identifying a novel MST4-LAMP2A signaling axis that regulates CMA activity and drives GSC stemness maintenance, tumor initiation and immune evasion in GBM. This pathway has not been described before and represents a significant conceptual advance, as it uncovers MST4 as a key upstream kinase that directly phosphorylates LAMP2A at residues T40, S97, and

T136. This post-translational modification facilitates multimerization of LAMP2A and enhances protein stability of lysosomal LAMP2A, thereby increasing LAMP2A abundance in lysosomes and CMA flux in GSCs. Our findings not only deepen the mechanistic understanding of CMA regulation but also propose MST4-LAMP2A as a druggable target for GSC-directed therapies.

2. **Mechanistic depth beyond prior studies.**

Our study moves beyond the descriptive correlations reported in earlier work (e.g., association of LAMP2A overexpression with elevated CMA activity in human GBM and GSCs, as well as the GSCs proliferation and tumorigenicity) to reveal precise molecular mechanisms. Through biochemical and functional assays, we demonstrated that MST4-mediated phosphorylation of LAMP2A disrupts its interaction with Cathepsin A, thereby stabilizing LAMP2A and sustaining CMA activity. These mechanistic insights—absent in prior studies—provide a foundation for targeting CMA in GSCs.

3. **Identification of two critical CMA-mediated pathways that are implicated in GSCs tumorigenicity and immune evasion.**

Although we leveraged OMIC datasets from Auzmendi-iriarte et al. as a starting point, our analysis expanded significantly by integrating transcriptomic and proteomic data to map CMA's functional network in GSC or GBM. This approach revealed two critical pathways regulated by CMA: (1) PI3K-AKT-mTORC1 signaling, where CMA promotes GSCs proliferation via lysosomal degradation of TSC1/2 (Core negative regulatory factors of mTOR1), and (2) cGAS-STING-mediated immune responses, where CMA suppresses antitumor immunity by degrading TET3, a DNA demethylase required for cGAS-STING activation. These findings resolve how CMA simultaneously sustains GSCs stemness and immune evasion—a dual role not previously appreciated.

4. **Scientific significance and translational impact**

Our study transcends prior observations by:

1) Establishing CMA as a master regulator of GSCs tumorigenicity, therapy resistance, and immune escape through novel molecular axes (MST4-LAMP2A, CMA-TSC1/2-mTORC1, CMA-TET3-cGAS/STING).
2) Providing the first evidence that MST4-mediated LAMP2A phosphorylation governs CMA activity and GSC stemness, and elucidating the role of CMA in shaping the immunosuppressive tumor microenvironment characteristic of GBM.
3) Demonstrating therapeutic synergy between CMA inhibition and existing treatments (e.g., anti-PD-1 immunotherapy, radiation), offering actionable strategies to combat therapy-resistant GBM.

5. **Suitability for *Nature Communications***

Our work addresses a critical gap in understanding how CMA mechanistically governs GSCs malignancy and therapy resistance. By uncovering novel regulatory layers (MST4 kinase-driven LAMP2A phosphorylation), resolving CMA's dual role in cancer stem cells and immunity, and proposing clinically relevant therapeutic combinations, our study holds broad relevance for cancer biologists, autophagy researchers, and translational oncologists. The mechanistic depth, multi-omics integration, and translational implications meet the journal's high standards for novelty, rigor, and interdisciplinary impact.

We firmly believe our study provides groundbreaking insights into CMA's role in GSCs, with sufficient novelty, mechanistic depth, and therapeutic relevance to warrant publication in *Nature Communications*. We sincerely appreciate your time and consideration and are fully committed to addressing any additional revisions to meet the journal's expectations. These insights bridge fundamental autophagy biology, cancer stem cells, and tumor immunology, aligning with *Nature Communications*' mission to publish interdisciplinary, high-impact research.

***Reviewer #4:***

*In the manuscript, the authors describe a novel mechanism of CMA regulation by stabilization of LAMP2A in the lysosome through its phosphorylation by MTS4. They also state that they have described two CMA targets that are implicated in GSC tumorigenicity: TCS1/2, implicated in mTOR1 pathway, and TET3, implicated in cGAS-STING pathway. Nevertheless, they don't clearly demonstrate that TET3 and TSC1/2 are CMA substrates, and that the effects they see in GSC tumorigenicity changes are only due to CMA modulation and not to macroautophagy. Importantly, there is not clear link between CMA regulation, effects they see in GSC tumorigenicity and the possible substrates, as they try to show this link only using a pharmacological modulator of CMA which might be none specific and also induce other cellular stress mechanisms.*

*The authors should address several major points to improve their study and meet the standards of the journal.*

**Response:** We sincerely appreciate the reviewer's insightful comments and constructive suggestions, which have significantly strengthened our manuscript. Below we provide point-by-point responses to each concern, with all recommended revisions implemented.

1) To validate TET3 and TSC1/2 as CMA substrates, we adhered strictly to established criteria (doi.org/10.1080/15548627.2020.1797280), which included:

- Identifying CMA-targeting motifs in TSC1/2 and TET3 utilizing the KFERQ Finder;
- Conducting CMA-specific degradation assays using the CMA inhibitor leupeptin and $NH_4Cl$ (LN), or silencing LAMP2A with shRNA;
- Performing immunofluorescence staining to assess the colocalization of TSC1/2 and TET3 with LAMP2A-positive lysosomes under CMA-inducing conditions (e.g., nutrient starvation);
- Conducting co-immunoprecipitation of TSC1/2 and TET3 with LAMP2A or HSC70/HSPA8.
- Carrying out *in vitro* CMA assays (binding and uptake) with CMA-active lysosomes and purified TSC1/2 or TET3 proteins, both with and without lysosomal protease inhibitors.

Further details regarding the validation of TSC1/2 and TET3 as CMA targets are included in our response to comment #2 from Reviewer #4.

2) To elucidate the specificity of CMA-related effects on alterations in GSC tumorigenicity, we examined the involvement of CMA in the degradation of TSC1/2 and its consequent impact on GSC tumorigenicity. This was accomplished by silencing endogenous TSC1/2 and subsequently reintroducing shRNA-resistant wild-type TSC1/2 alongside variants with mutations in the HSC70 binding motif. Under standard culture conditions, neither the silencing nor the reintroduction of

TSC1/2 exhibited significant modifications in macroautophagy levels, as evidenced by stable LC3-II/I ratios and p62 concentrations. Conversely, the knockdown of ATG5, serving as a control for macroautophagy deficiency, induced a reduction in LC3-II conversion and an increase in p62 accumulation. TSC1/2 silencing promoted GSC proliferation and spheroid formation, while reintroducing wild-type and mutant (HSC70-binding motif variants) TSC1/2 reversed these effects, with mutants showing greater tumorigenicity suppression. Importantly, TSC1/2's modulation of mTORC1 activity did not affect GSC macroautophagy, implying that TSC1/2 influences GSC tumorigenicity via CMA, not macroautophagy.

Further details regarding the alterations in GSC tumorigenicity attributable solely to CMA modulation, independent of macroautophagy, are elaborated in our response to comment #5 from Reviewer #4.

3) To address the concern regarding the ambiguous relationship between CMA regulation, GSC tumorigenicity, and potential substrates, we performed knockdown experiments targeting endogenous Mst4 or Lamp2a in murine syngeneic glioblastoma cell lines CT-2A and GL261. This intervention resulted in a substantial upregulation of CMA substrates TET3 and TSC1/2 (PBP Fig. 7a). Subsequent intracranial implantation of these genetically modified cells into immunocompetent C57BL/6 mice revealed that the ablation of Mst4 or Lamp2a significantly curtailed tumor growth and prolonged animal survival (PBP Fig. 7b-e), concurrently enhancing the expression of CMA substrates TET3 and TSC1/2 within the tumors, as demonstrated by immunofluorescence analysis of murine tissues (PBP Fig. 7f). Furthermore, xenografts treated with the CMA inhibitor PPD showed increased levels of TET3 and TSC1/2, suggesting that PPD effectively penetrates the blood-brain barrier (BBB) and mitigates tumorigenicity by inhibiting the CMA-mediated degradation of TET3 and TSC1/2 in the xenografts (PBP Fig. 7g-j).

These results are shown in revised Fig. 9b-e, g-h and Supplementary Fig. 9b-c, l-m, with detailed descriptions provided on page 27-29 (line 581-609 and 611-615).

While PPD is found as a CMA-targeting inhibitor (Dong, Rui-Fang et al. *Br J Pharmacol.* 2025;182(10):2287-2309.), its specificity may be compromised as it can influence other cellular stress pathways (Wang, Yang et al. *Mol Ther*. 2023;31(7):2169-2187.). This highlights a broader issue in the field, given the scarcity of highly selective CMA inhibitors (Kaushik S, Cuervo AM. *Nat Rev Mol Cell Biol*. 2018;19(6):365-381.). The recent discovery of CIM7 (McCabe, Mericka et al. *EMBO Mol Med*. Published online June 9, 2025.), which inhibits CMA without affecting macroautophagy, marks a significant progress and positions CIM7 as a strong candidate for future research on CMA-targeted therapies for GBM, potentially overcoming PPD's limitations. We have incorporated this information into the discussion of the revised manuscript (page 34, line 721-727).

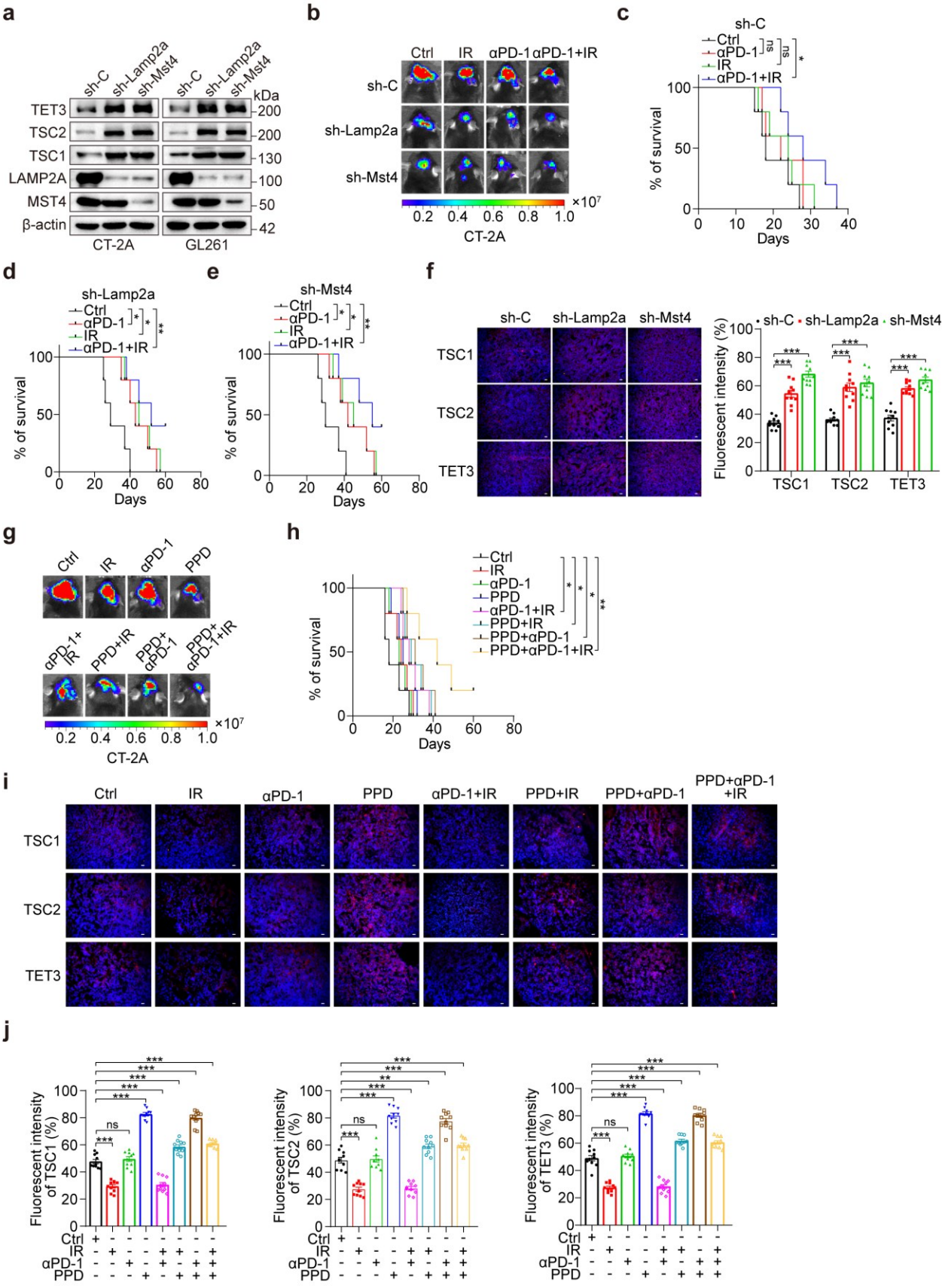
a
sh-C
sh-Lamp2a
sh-Mst4
kDa
TET3
TSC2
TSC1
LAMP2A
MST4
β-actin
CT-2A
GL261
b
Ctrl
IR
αPD-1
αPD-1+IR
sh-C
sh-Lamp2a
sh-Mst4
CT-2A
c
sh-C
Ctrl
αPD-1
IR
αPD-1+IR
% of survival
Days
d
sh-Lamp2a
e
sh-Mst4
f
TSC1
TSC2
TET3
Fluorescent intensity (%)
g
PPD
PPD+IR
PPD+αPD-1
PPD+αPD-1+IR
h
PPD+αPD-1
PPD+αPD-1+IR
i
j
Fluorescent intensity of TSC1 (%)
Fluorescent intensity of TSC2 (%)
Fluorescent intensity of TET3 (%)

**PBP Fig. 7 a:** IB analyses for indicated proteins in CT-2A and GL261 cells expressing sh-C, sh-Lamp2a or sh-Mst4.

**PBP Fig. 7 b:** Representative luciferase-based bioluminescence images of C57BL/6 mice with intracranially transplanted CT-2A cells with indicated modifications and treatments. Colored scale bars represent photons/s/cm$^2$/steradian.

**PBP Fig. 7 c-e:** Kaplan-Meier survival curves of C57BL/6 mice with intracranially transplanted with CT-2A cells with modifications and treatments. n = 5/group.

**PBP Fig. 7 f:** Representative IF staining images (left) and quantification (right) for fluorescent intensity of TSC1, TSC2 and TET3 in tumor tissues from C57BL/6 mice with intracranial CT-2A cells transplants with indicated modifications. Data are presented as the mean ± S.E.M. n = 10 randomly selected microscopic fields. Scale bar, 20 μm.

**PBP Fig. 7 g:** Representative luciferase-based bioluminescence images of C57BL/6 mice with intracranially transplanted CT-2A cells with indicated treatments. Colored scale bars represent photons/s/cm$^2$/steradian.

**PBP Fig. 7 h:** Kaplan-Meier survival curves of C57BL/6 mice with intracranially transplanted with CT-2A cells with indicated treatments. n = 5/group.

**PBP Fig. 7 i-j:** Representative IF staining images (**i**) and quantification (**j**) for fluorescent intensity of TSC1, TSC2 and TET3 in tumor tissues from C57BL/6 mice with intracranial CT-2A cells transplants with indicated modifications. Data are presented as the mean ± S.E.M. n = 10 randomly selected microscopic fields. Scale bar, 20 μm.

Statistical significance was assessed using log-rank test (**c**, **d**, **e**, **h**) or one-way ANOVA with Dunnett's multiple comparisons test (**f**, **j**). ns, not significant. *$p$ < 0.05, **$p$ < 0.01, ***$p$ < 0.001.

*1. The authors state in the introduction: "MST4 is recognized for phosphorylating ATGB4, thereby initiating macroautophagy, which enhances cell survival and tumorogenic potential of GSCs". However, when they regulate MST4 levels, they only attribute changes in GCS tumorigenicity to changes in CMA without showing if also levels of macroautophagy are changed (LC3 flux). They must show if macroautophagy is implicated in MST4 regulation of tumorgenicity.*

**Response:** We sincerely appreciate the reviewer's insightful critique regarding the potential roles of macroautophagy and CMA in MST4-mediated tumorigenicity. To address this, we systematically evaluated both autophagy pathways through complementary experiments. In gain-of-function studies using MST4-deficient GSC 23 cells, ectopic MST4 expression not only elevated CMA activity, as evidenced by increased PA-mCherry-KFERQ puncta and reduced levels of CMA substrates (MEF2D: 0.54-fold decrease; GAPDH: 0.43-fold decrease; PBP Fig. 8a, b), but also enhanced macroautophagy. The latter was demonstrated by three independent markers: (i) elevated LC3-II/LC3-I ratio (PBP Fig. 8a), (ii) accelerated p62 degradation (PBP Fig. 8a), and (iii) increased LC3B puncta/cell (PBP Fig. 8c).

Notably, pathway-specific inhibition revealed compensatory crosstalk between macroautophagy and CMA: ATG4B knockdown (macroautophagy blockade) paradoxically increased CMA activity in MST4-overexpressing cells (PBP Fig. 8b). Conversely, LAMP2A knockdown (CMA inhibition) upregulated macroautophagy flux in MST4-overexpressing cells (PBP Fig. 8c).

In xenograft models, knockdown of ATG4B or LAMP2A reduced MST4-driven tumor growth by 73% and 68% ($p$ < 0.001), respectively (PBP Fig. 8d, e). Combined ATG4B/LAMP2A inhibition

synergistically reduced tumor burden by 97% ($p < 0.001$; PBP Fig. 8d, e) and extended median survival from 16 days (MST4 overexpression) to 45 days ($p < 0.01$; PBP Fig. 8f). Immunofluorescence confirmed that MST4 overexpression increased both LC3B and LAMP2A signals. ATG4B knockdown increased LAMP2A levels, while LAMP2A knockdown boosted LC3B flux, mirroring the crosstalk seen *in vitro* (PBP Fig. 8g-i).

Our findings show that MST4 activate both macroautophagy and CMA in GSCs, with compensatory crosstalk between the pathways. This interdependence highlights the potential of dual autophagy inhibition for overcoming treatment resistance. Supplementary Fig. 4h-p have been updated to reflect these results with detailed descriptions appearing on page 16-17, line 343-351.

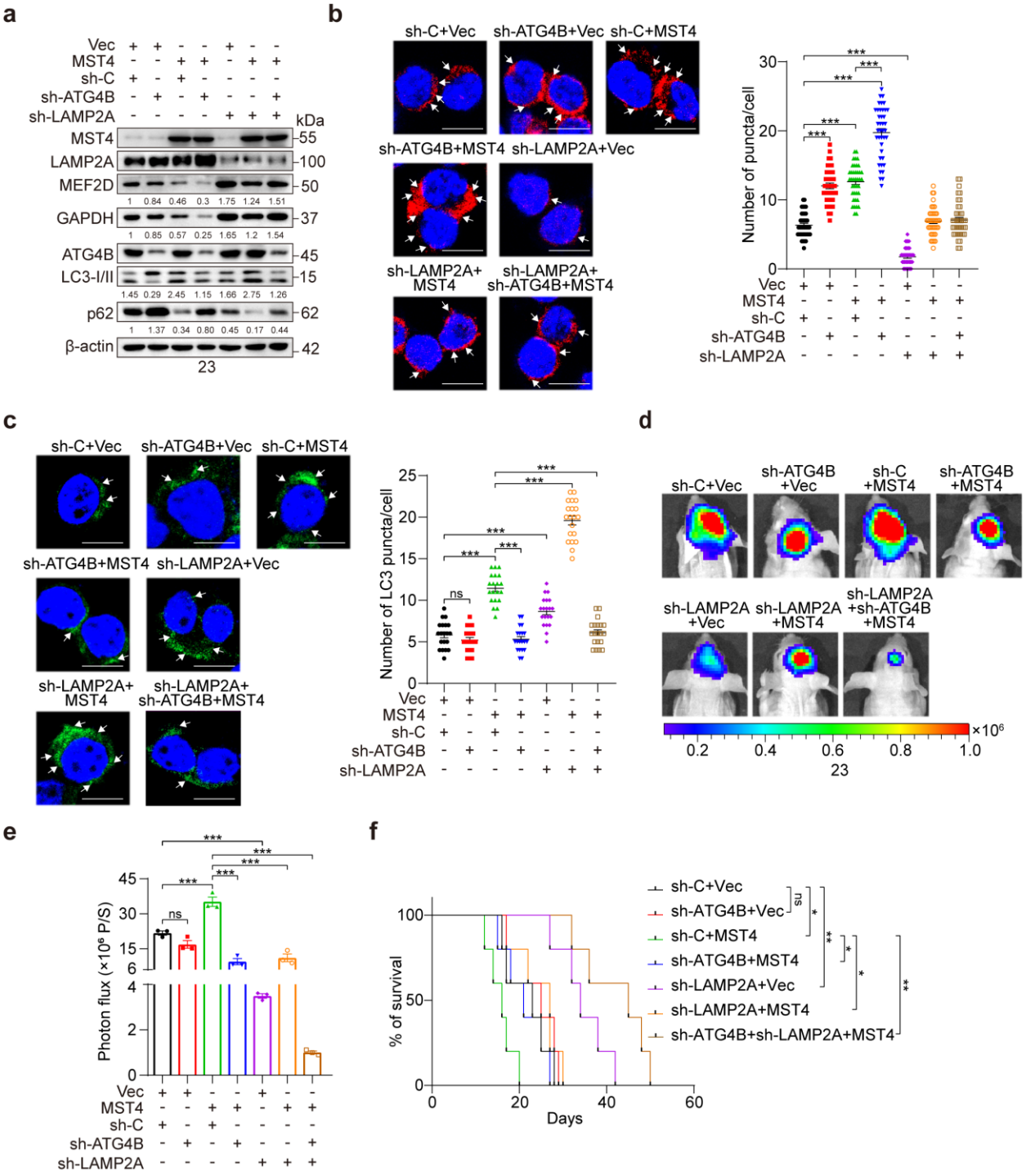
a
Vec
MST4
sh-C
sh-ATG4B
sh-LAMP2A
kDa
MST4
LAMP2A
MEF2D
GAPDH
ATG4B
LC3-I/II
p62
β-actin
23
b
sh-C+Vec
sh-ATG4B+Vec
sh-C+MST4
sh-ATG4B+MST4
sh-LAMP2A+Vec
sh-LAMP2A+ MST4
sh-LAMP2A+ sh-ATG4B+MST4
Number of puncta/cell
c
sh-C+Vec
sh-ATG4B+Vec
sh-C+MST4
sh-ATG4B+MST4
sh-LAMP2A+Vec
sh-LAMP2A+ MST4
sh-LAMP2A+ sh-ATG4B+MST4
Number of LC3 puncta/cell
d
sh-C+Vec
sh-ATG4B +Vec
sh-C +MST4
sh-ATG4B +MST4
sh-LAMP2A +Vec
sh-LAMP2A +MST4
sh-LAMP2A +sh-ATG4B +MST4
×10⁶
23
e
Photon flux (×10⁶ P/S)
f
% of survival
Days
sh-C+Vec
sh-ATG4B+Vec
sh-C+MST4
sh-ATG4B+MST4
sh-LAMP2A+Vec
sh-LAMP2A+MST4
sh-ATG4B+sh-LAMP2A+MST4
g
sh-C+Vec
sh-ATG4B +Vec
sh-C +MST4
sh-ATG4B +MST4
sh-LAMP2A +Vec
sh-LAMP2A +MST4
sh-LAMP2A +sh-ATG4B +MST4
LAMP2A
LC3B

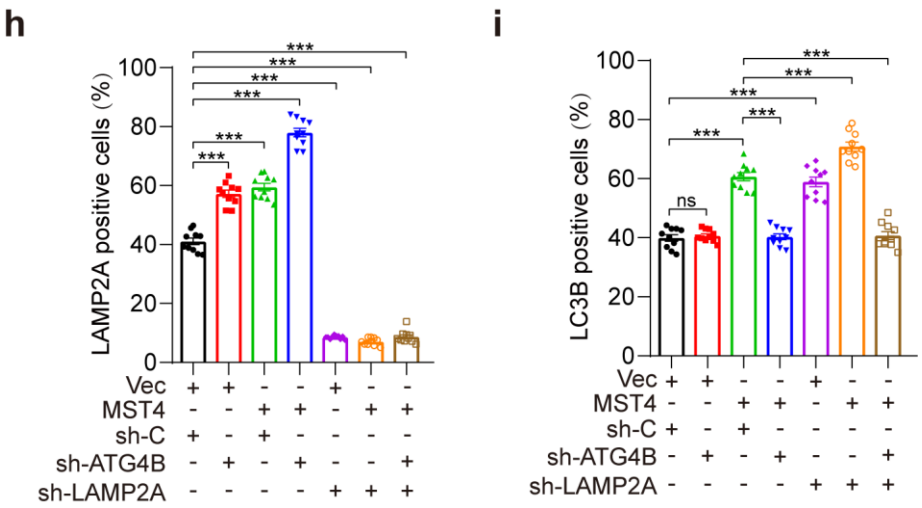


**PBP Fig. 8 a:** IB analyses for indicated proteins in GSC 23 cells with indicated modifications. Quantifications in ratios of MEF2D, GAPDH, p62 relative to β-actin, as well as LC3B-II:-I ratios are shown.

**PBP Fig. 8 b:** Representative images (left) and quantification (right) of CMA activity detection by KFERQ puncta frequency in GSC 23 cells with indicated modifications. Data are presented as the means ± S.E.M. n = 40 randomly selected cells. Scale bar, 10 μm.

**PBP Fig. 8 c:** Representative images (left) and quantification (right) of IF staining analyses of LC3B puncta frequency in GSC 23 cells with indicated modifications. Data are presented as the means ± S.E.M. n = 20 randomly selected cells. Scale bar, 10 μm.

**PBP Fig. 8 d:** Representative luciferase-based bioluminescence images of athymic (BALB/c Nude) mice with intracranially transplanted GSC 23 cells with indicated modifications. Colored scale bars represent photons/s/cm$^2$/steradian.

**PBP Fig. 8 e:** Quantification of tumor bioluminescence of mice in d. Data are presented as the means ± S.E.M. n = 3.

**PBP Fig. 8 f:** Kaplan-Meier survival curves of athymic (BALB/c Nude) mice with intracranially transplanted with GSC 23 cells with indicated treatments. n = 5/group.

**PBP Fig. 8 g-i:** Representative images (**g**) and quantification (**h**, **i**) of IF staining for LC3B and LAMP2A positive cells in tumor tissues from BALB/c Nude mice intracranially transplanted with GSC 23 cells with indicated modifications. Data are presented as the means ± S.E.M. n = 10 randomly selected microscopic fields.

Statistical significance was assessed using one-way ANOVA with Dunnett's multiple comparisons test (h), one-way ANOVA with Tukey's multiple comparisons test (**b**, **c**, **e**, **i**) or log-rank test (**f**). ns, not significant. *$p$ < 0.05, **$p$ < 0.01, ***$p$ < 0.001.

*2. Authors do not follow all the known guidelines to validate their potential CMA substrates, therefore, they are not showing that MST4 and TET3 are CMA substrates (doi.org/10.1080/15548627.2020.1797280).*

**Response:** We thank the reviewer for highlighting the importance of rigorously validating CMA substrates. We acknowledge the guidelines outlined in the referenced literature (doi.org/10.1080/15548627.2020.1797280) and confirm that our experimental approach aligns with key criteria for identifying CMA substrates, as detailed below:

1) Identification of CMA-Targeting Motifs: As recommended, we first analyzed the amino acid sequences of TSC1/2 and TET3 for the presence of KFERQ-like motifs using the KFERQ Finder (Philipp Kirchner, et al. *PLoS Biol*. 2019 May 31;17(5): e3000301.). We found that TSC1/2 has two canonical KFERQ-like motifs, and TET3 protein have five (PBP table 1). These motifs were further validated by mutagenesis experiments, where disruption of the motifs (e.g., alanine substitution) significantly reduced their degradation rates in CMA-active conditions (PBP Fig. 9a-d).

PBP table 1 KFERQ-like motifs in indicated proteins.

| Protein names | Canonical KFERQ motif | position | mutation |
|---|---|---|---|
| TSC1 | DRLIQ | [650:654] | DALIQ |
| TSC1 | DVKLQ | [932:936] | DVALQ |
| TSC2 | RKELQ | [350:354] | AAELQ |
| TSC2 | ERLLQ | [366:370] | EALLQ |
| TET3 | ELIRQ | [574:578] | ELIAQ |
| TET3 | QIKIE | [621:625] | QIAIE |
| TET3 | QIVEK | [698:702] | QIVEA |
| TET3 | QKEKL | [1042:1046] | QAEAL |
| TET3 | EKIKQ | [1050:1054] | EAIAQ |

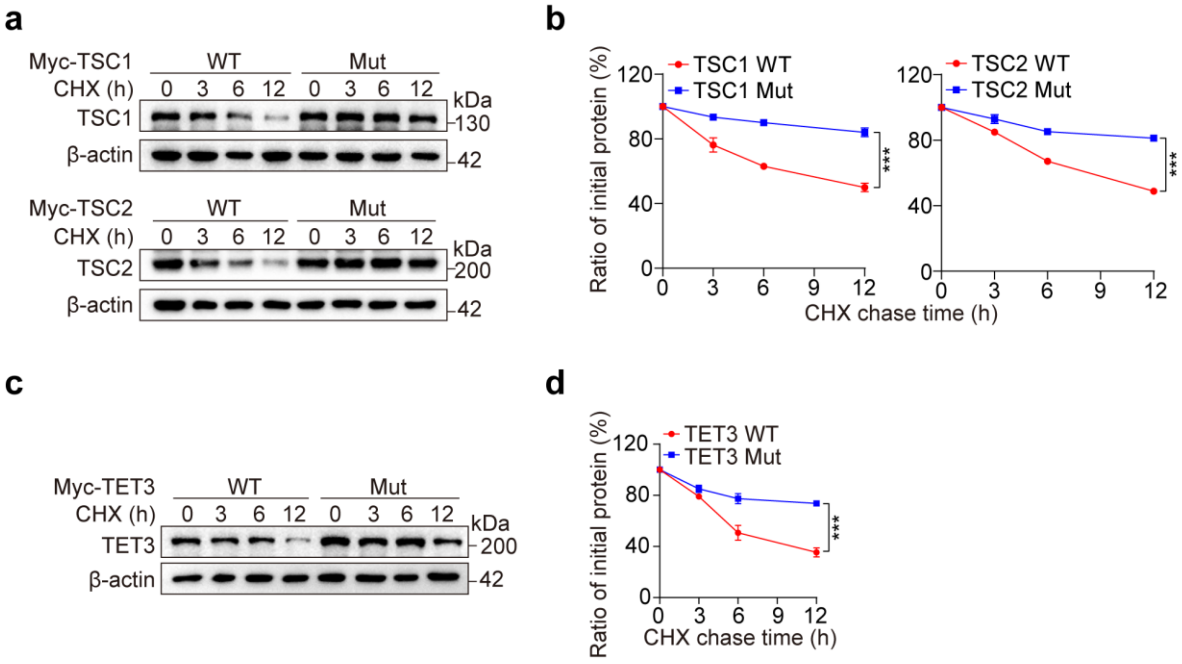

**PBP Fig. 9 a, c:** IB for TSC1, TSC2 and TET3 in HEK293T cells subjected to indicated modifications, subsequently treated with cycloheximide (CHX) (100 μg/mL) for the indicated time.

**PBP Fig. 9 b, d:** Quantification of TSC1, TSC2 and TET3 protein levels in HEK293T cells with indicated modifications and treatments. Data are presented as the means ± S.E.M. n = 3 independent experiments. Statistical significance was assessed using Bonferroni's multiple comparisons test. ***$p$ < 0.001.

2) CMA-Specific Degradation Assays: To confirm CMA-dependent degradation of TSC1/2 and TET3, we performed CMA inhibition by treatment with leupeptin and $NH_4CL$ (LN). Western blot showed that the degradation of TSC1/2 and TET3 was inhibited by LN treatment. Compared with LN treatment, inhibition of macroautophagy via 3-methyladenine (3-MA) or proteasomal inhibition with MG132 did not alter the expression of TSC1/2 and TET3 in HEK293T cells (PBP Fig. 10a, b). Furthermore, shRNA-mediated silencing of LAMP2A, a CMA-limiting component, markedly reduced TSC1/2 and TET3 degradation (PBP Fig. 10c-f), whereas the overexpression of LAMP2A-WT or -3D, as opposed to -3A or -4A, markedly accelerated their degradation, (PBP Fig. 10g, h), indicating that the lysosomal degradation of TSC1/2 and TET3 requires the presence of LAMP2A.

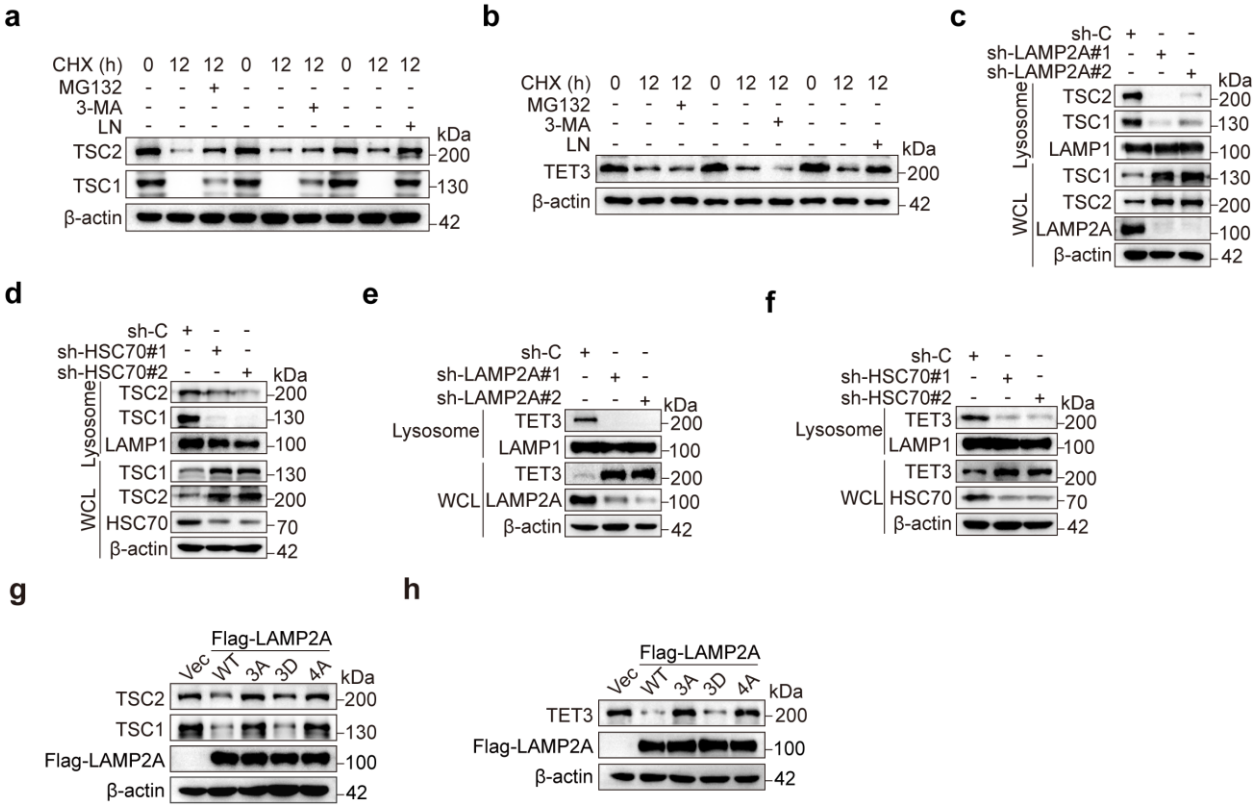


**PBP Fig. 10 a, b:** IB analyses for TSC1, TSC2 or TET3 in GSC M83 cells, either untreated or subjected to 10 μM MG132, 5 mM 3-MA or LN (10 μM leupeptin and 20 mM $NH_4Cl$) for an additional 12 hours post-CHX (100 μg/mL) treatment for 12 hours.

**PBP Fig. 10 c-f:** IB analyses for TSC1/2 or TET3 protein levels in WCL and lysosomal fractions of GSC M83 cells, with or without LAMP2A KD (**c**, **e**) or HSC70 KD (**d**, **f**).

**PBP Fig. 10 g, h:** IB analyses for TSC1, TSC2 or TET3 in HEK293T cells with or without overexpressing Flag-LAMP2A-WT or mutants.

3) Colocalization with Lysosomal Compartments: We performed immunofluorescence staining and found colocalization of TSC1/2 and TET3 with LAMP2A-positive lysosomes under CMA-inducing conditions (e.g., nutrient starvation) (PBP Fig. 11a-c). This lysosomal association was abolished upon mutagenesis of the KFERQ motifs (PBP Fig. 11a-c).

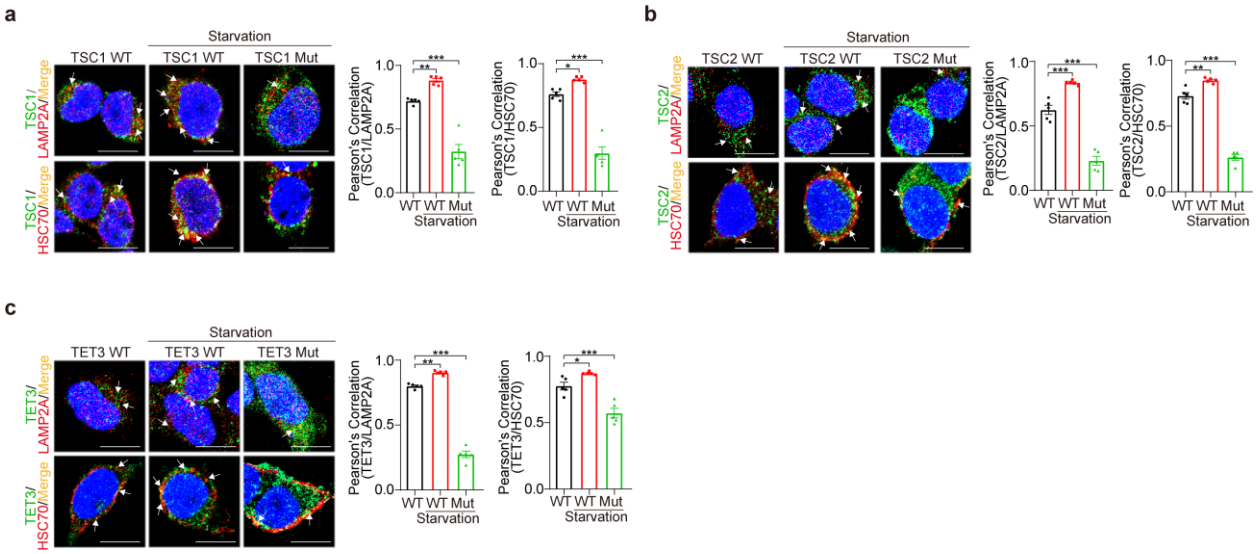


**PBP Fig. 11 a-c:** IF staining analyses of HEK293T cells overexpressing Myc-TSC1 (**b**), Myc-TSC2 (**c**) or Myc-TET3 (**g**) using anti-LAMP2A or HSC70 and anti-Myc antibodies, with or without starvation treatment. Myc-TSC1/TSC2/TET3 (green), LAMP2A or HSC70 (red), DAPI (blue). Scale bar, 10 μm. The right panel is the quantification of Pearson's correlation between TSC1/TSC2/TET3 and LAMP2A or HSC70. Data are presented as the means ± S.E.M. n = 5 randomly selected cells. Statistical significance was assessed using one-way ANOVA with Dunnett's multiple comparisons test. *$p < 0.05$, **$p < 0.01$, ***$p < 0.001$.

4) Co-immunoprecipitation of TSC1/2 or TET3 with LAMP2A or HSC70/HSPA8: We performed Co-immunoprecipitation of TSC1/2 or TET3 and found association of wild-type TSC1/2 or TET3 with LAMP2A or HSC70/HSPA8 was decreased upon mutagenesis of the KFERQ motifs in TSC1/2 or TET3 (PBP Fig. 12a-c).

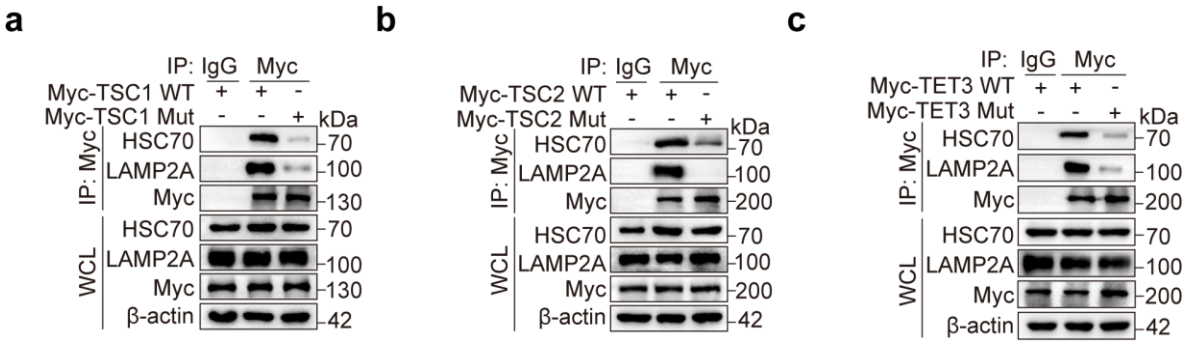


**PBP Fig. 12 a-c:** IP-IB analyses for indicated proteins in HEK293T cells transduced with the indicated plasmids.

5) *In Vitro* CMA Reconstitution: as suggested in the guidelines, we performed *in vitro* CMA assays using CMA active lysosomes isolated from HEK293T cells. Purified TSC1/2 or TET3 proteins was incubated with lysosomes untreated or previously incubated with inhibitors of lysosomal proteases. Immunoblotting of recovered lysosomes showed that TSC1/2 or TET3 uptake and degraded by lysosomes (PBP Fig. 13a-d).

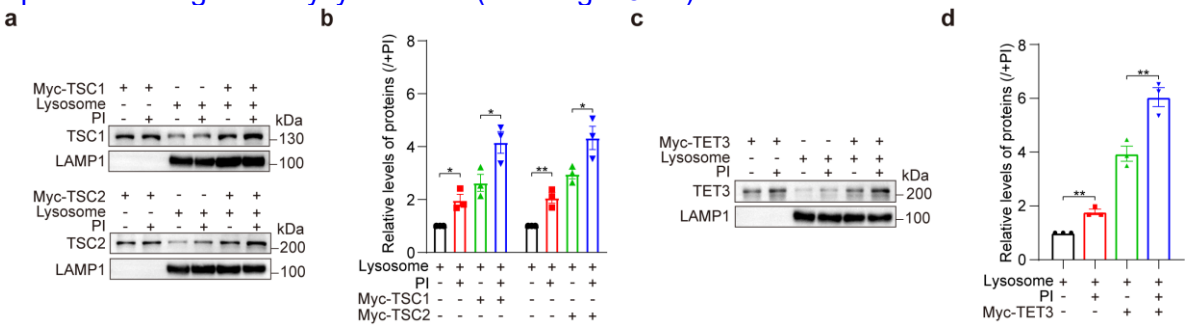


**PBP Fig. 13 a, c:** *In vitro* lysosomal uptake assay of TSC1, TSC2 (a) or TET3 (c). Following co-incubation with lysosomes isolated from HEK293T cells in the presence or absence of protease inhibitors (PI), Myc-TSC1/TSC2/TET3 were internalized and degraded by lysosomes. An empty lysosome sample served as the negative control, while substrate-only reactions (without lysosomes) were included as input controls. LAMP1 was used to demonstrate equal lysosomal loading.
**PBP Fig. 13 b, d:** Quantification of TSC1, TSC2 (**b**) or TET3 (**c**) levels. Data are presented as the means ± S.E.M. n = 3 independent experiments. Statistical significance was assessed using two-tailed Student's t-test. *$p < 0.05$, **$p < 0.01$.

Our experimental workflow rigorously adheres to established criteria for CMA substrate validation, including motif identification, degradation assays, lysosomal colocalization, and functional reconstitution. Collectively, these lines of evidence supported TSC1/2 or TET3 as the targets of CMA. We appreciate the reviewer's emphasis on comprehensive validation.

Additional supporting Data were presented in revised Supplementary Table 1, Figures 5, 7 and Supplementary Figures 5, 7, with detailed explanations provided on page 18-19, line 378-402 and page 24-25, line 507-529. The newly developed experimental protocol has been incorporated into the Methods section (*In vitro* lysosome binding and uptake assay) on page 52, line 1104-1109.

*3. Authors must show the quality of lysosome preparations. They should show enrichment of LAMP1 or LAMP2A in the lysosome lysates vs whole cell lysates by WesternBlot. Moreover, they must show the quality of the lysosomal preparations, showing absence of mitochondrial and cytosolic markers in their Western-blot with lysosomal preparations.*

**Response:** We sincerely appreciate the reviewer's valuable suggestion regarding the quality control of lysosomal preparations. We performed validation of our lysosome isolation protocol using GSC 23, M83, and 456 cells, following established methods from the previous publication (Caballero et al., *Nat Commun* 2021). Western blot analysis demonstrated a marked enrichment of the lysosomal marker LAMP1 in purified lysosomal fractions relative to whole-cell lysates, along with concomitant enrichment of HSC70 - a critical chaperone for chaperone-mediated autophagy (CMA) (PBP Fig. 14a-e). Importantly, our quality control assays confirmed the absence of detectable mitochondrial (COX IV) and cytosolic (β-actin) contaminants in the lysosomal preparations, confirming preparation purity (PBP Fig. 14a-e).

These Data were included in Fig. 4a, i and Supplementary Fig. 4a, b, e, along with page 15, line 303-316 and page 16, line 324-327, and Lysosomes isolation in Methods section (page 51, line 1086-1087) of the revised manuscript.

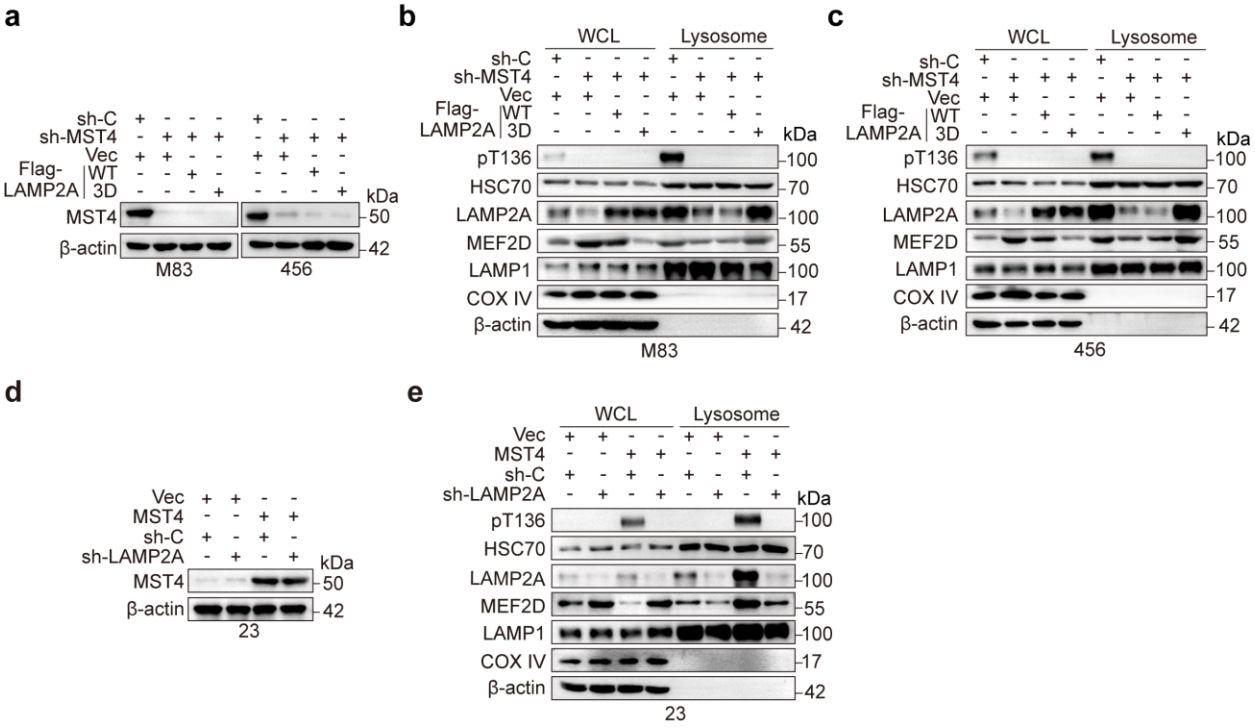


**PBP Fig.14 a, d:** IB analyses for indicated proteins in GSC M83, GSC 456, and GSC 23 cells with indicated modifications.

**PBP Fig.14 b, c, e:** IB analyses for indicated proteins in WCL and lysosomal fractions of GSC M83, GSC 456, and GSC 23 cells with indicated modifications.

*4. Authors must clearly demonstrate that lysosomes are CMA competent: they should see an increase in HSC70 and not only in LAMP2A levels in WB to conclude there's an activation of CMA. They should corroborate that those CMA competent lysosomes have increased phosphorylated LAMP2A when modifying MST4 levels.*

**Response:** We appreciate the reviewer for pointing out this important issue. We isolated lysosomes from GSC 23, M83, and 456 cells using established methods as described in the previous publication (Caballero *et al*., *Nat Commun* 2021). Western blot analysis revealed a substantial enrichment of HSC70 in the purified lysosomal fractions compared to whole-cell lysates (PBP Fig.15 a-e). Notably, MST4 overexpression in GSC 23 resulted in a significant increase in both p-LAMP2A and total LAMP2A levels within the lysosomes. Furthermore, LAMP2A knockdown effectively abolished the MST4-induced accumulation of p-LAMP2A (PBP Fig.15 a-b). In contrast, MST4 knockdown in M83 and 456 cells led to decreased levels of p-LAMP2A and reductions in lysosomal LAMP2A; however, HSC70 levels remained unchanged (PBP Fig.15 c-e). Interestingly, the phosphomimetic variant of LAMP2A (3D) was able to restore the diminished lysosomal levels of LAMP2A resulting from MST4 deletion (PBP Fig.15 c-e). These

findings suggest that MST4-mediated phosphorylation of LAMP2A enhances its enrichment within lysosomes and activates CMA.

The new results were presented as Fig. 4a, i and Supplementary Fig. 4a, b, e, with detailed methodological information provided in page 15, line 303-316 and page 16, line 324-327, of the revised manuscript.

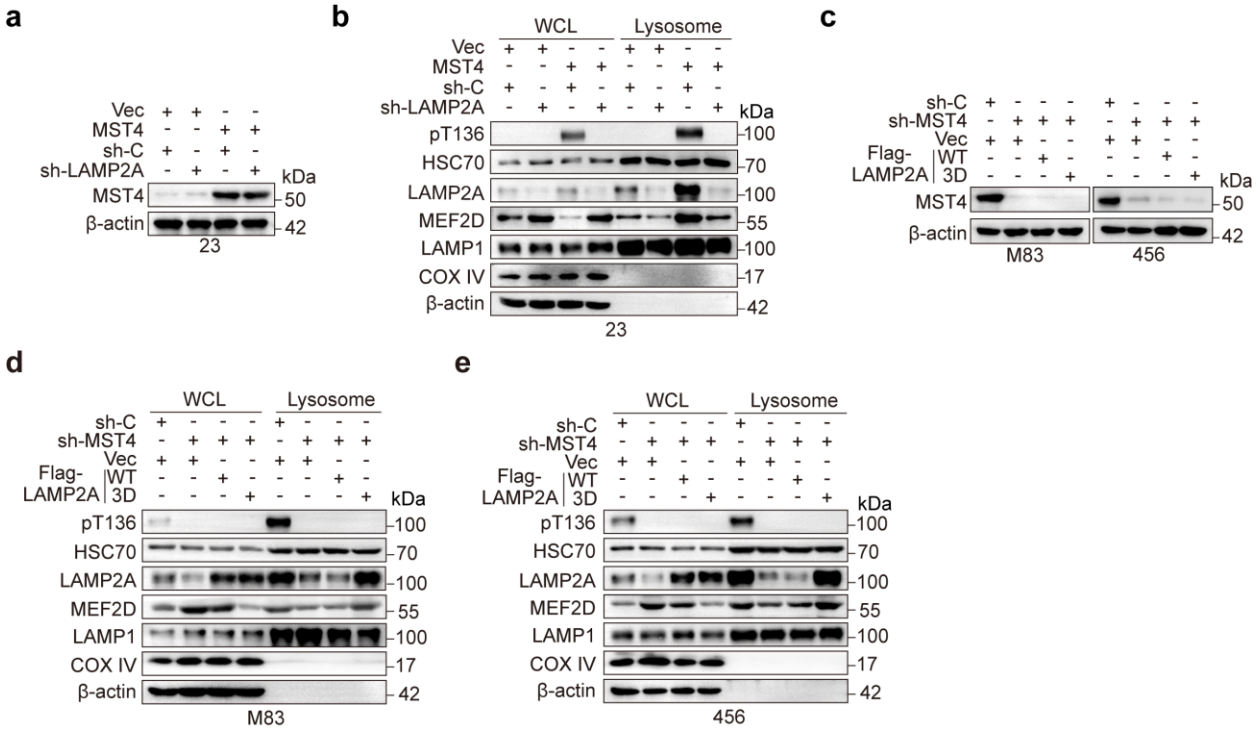


**PBP Fig. 15 a, c:** IB analyses for indicated proteins in WCL of GSC 23, GSC 83 and GSC 456 cells with indicated modifications.

**PBP Fig. 15 b, d, e:** IB analyses for indicated proteins in WCL and lysosomal fractions of GSC 23, GSC 83 and GSC 456 cells with indicated modifications.

*5. TCS1/2 is a known regulator of macroautophagy. Authors should prove that regulation of TCS1/2 does not alter macroautophagy levels, so that the effects on GCS that they see in tumorigenicity are caused only by CMA regulation.*

**Response:** We appreciate the reviewer's insightful comment regarding TSC1/2's potential roles in regulation of macroautophagy. To address this, we systematically evaluated macroautophagy activity under three experimental conditions: (1) TSC1/2 knockdown, (2) rescue with shRNA-resistant WT or CMA-resistant (KFERQ-mutant) TSC1/2, and (3) ATG5 knockdown as a macroautophagy-deficient control.

Key findings demonstrate that neither TSC1/2 manipulation (knockdown or rescue) altered LC3-II/I ratios or p62 levels, while ATG5 knockdown showed expected macroautophagy impairment (PBP Fig. 16a). Intriguingly, intracranial xenografts revealed: (1) Rescue of CMA-resistant TSC1/2

mutants significantly decreased tumorigenicity compared to TSC1/2 wild-type (PBP Fig. 16b); (2) Equivalent LC3B expression in TSC1/2-modulated tumors versus controls, while significant LC3B reduction in ATG5-knockdown tumors ($p < 0.001$; PBP Fig. 16c). Taken together, these results suggest that modulation of TCS1/2 by CMA does not alter macroautophagy levels.

Mechanistically, TSC1/2 knockdown enhanced mTORC1 signaling (increased p-P70S6K/p-4EBP1) and tumor growth, effects reversed by TSC1/2 re-expression with mutant superiority (PBP Fig. 16a-c). Crucially, ATG5 knockdown did not affect mTORC1 activity, confirming CMA-specific regulation of the mTORC pathway (PBP Fig. 16a-c).

These comprehensive data establish that TSC1/2's tumorigenic effects in GSCs operate exclusively through CMA-mediated mTORC1 regulation, independent of macroautophagy modulation.

These results are now included in the updated Fig. 5 k and Supplementary Fig. 5 m-o, as described on page 19-20, line 409-425.

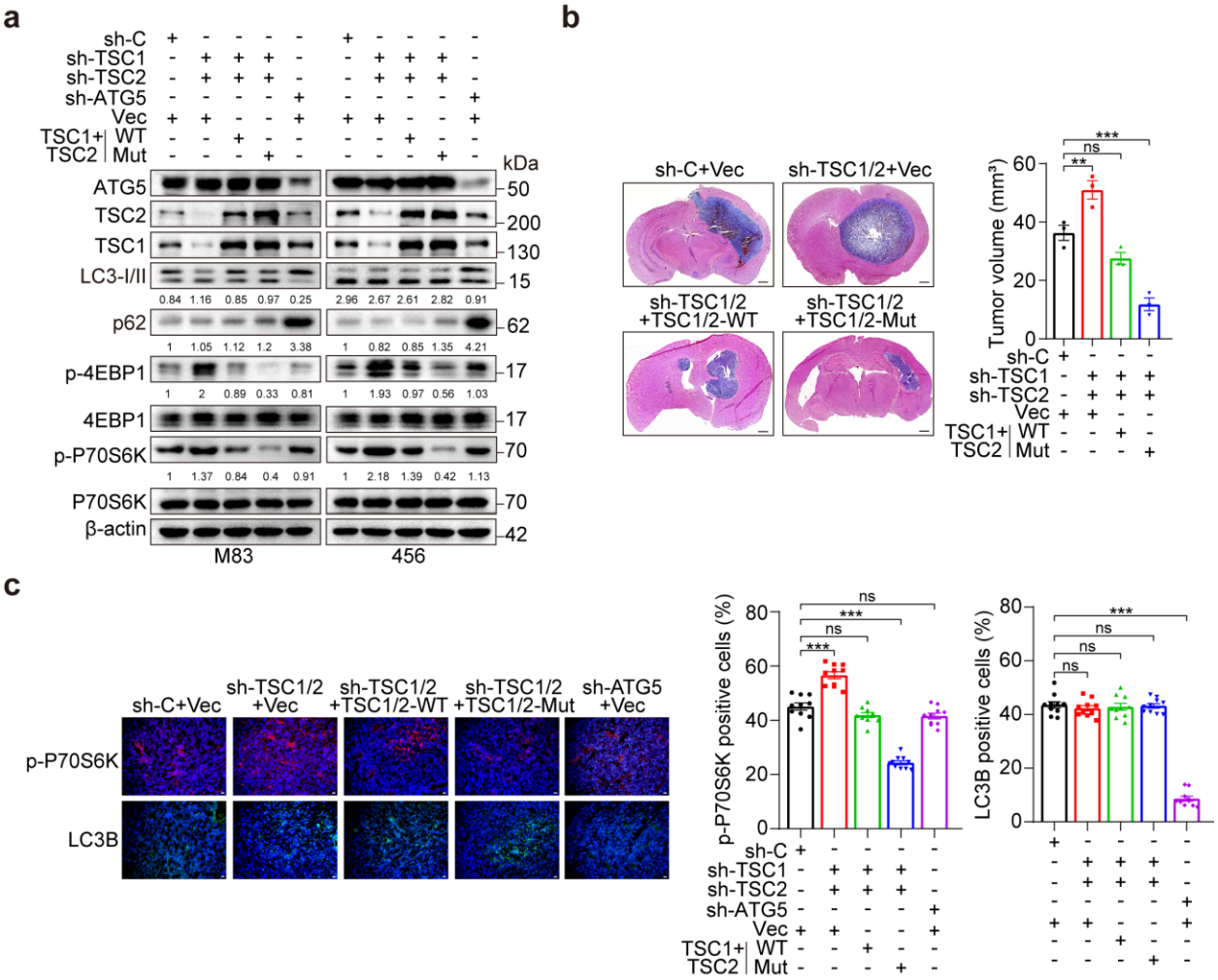

**PBP Fig. 16 a:** IB analyses for indicated proteins in GSC M83 and 456 cells with indicated modifications. Quantifications in ratios of p-4EBP1, p-P70S6K, p62 relative to β-actin, as well as LC3B-II:-I ratios are shown.

**PBP Fig. 16 b:** Representative H&E images of mouse brain sections (left) and quantification of tumor volume (right) from athymic (BALB/c Nude) mice intracranially implanted with GSC M83 cells with indicated modifications. Data are presented as the means ± S.E.M. n = 3. Scale bar, 1.0 mm.

**PBP Fig. 16 c:** Representative images (left) and quantification (right) of IF staining for LC3B and p-P70S6K expression in tumor tissues from BALB/c Nude mice intracranially transplanted with GSC M83 cells with indicated modifications. Data are presented as the means ± S.E.M. n = 10 randomly selected microscopic fields.

Statistical significance was assessed using one-way ANOVA with Dunnett's multiple comparisons test (**b**, **c**). ns, not significant. $^{**}p < 0.01$, $^{***}p < 0.001$.

*6. Besides all the above recommendations to validate CMA substrates, authors also should validate that TET3 expression they see is due to changes in protein levels and not due to gene expression (measuring mRNA levels).*

**Response:** We thank the reviewer for this insightful suggestion. To address whether TET3 regulation occurs at the protein versus transcriptional level, we performed qPCR analysis under CMA inhibition conditions. As shown in PBP Fig. 17a and b, neither LAMP2A knockdown nor HSC70 depletion induced significant changes in *TET3* mRNA levels ($p > 0.05$ by one-way ANOVA with Dunnett's multiple comparisons test). This demonstrates that the altered TET3 protein expression observed following CMA modulation results from post-translational regulation rather than transcriptional changes, consistent with CMA's established role in protein degradation. These findings further support our conclusion that TET3 is a bona fide CMA substrate.

Supplementary Fig. 7d and e have been updated to reflect these results, and detailed descriptions are provided on page 24, line 516-517 of the manuscript.

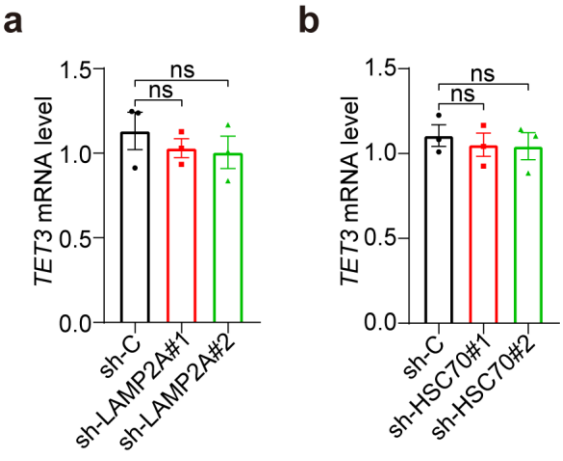


**PBP Fig. 17 a, b:** qPCR assessment of mRNA level of *TET3* in HEK293T cells with or without LAMP2A (**a**) or HSC70 (**b**) knock down. Data are presented as the means ± S.E.M. n = 3 independent experiments.

Statistical significance was assessed using one-way ANOVA with Dunnett's multiple comparisons test. ns, not significant.

*7. If authors are able to demonstrate that TET3 and TCS1/2 are CMA substrates, they should show if the increased stability of the phosphorylated LAMP2A at the lysosomal membrane is a common mechanism among other types of cells, not only in GSCs. They should include a model where CMA is downregulated (for example an aging model) and test whether they can restore CMA by introducing the phosphomimic version they use.*

**Response:** Thank you for this insightful suggestion. To address whether the increased stability of phosphorylated LAMP2A at the lysosomal membrane represents a common mechanism across cell types, we extended our analysis to human MRC-5 fibroblasts. Specifically, we compared the half-life of LAMP2A and the levels of phosphorylated LAMP2A in lysosomal membranes between early-passage (P18) and late-passage (P45) fibroblasts (PBP Fig. 18a-c). Although cell passage does not recapitulate all aspects of aging, senescent fibroblasts in culture have been shown to mirror CMA alterations observed in aged rodents, including reduced CMA activity and lower lysosomal LAMP2A levels (A M Cuervo & J F Dice. *J Biol Chem*. 2000;275(40):31505-13.). While late-passage fibroblasts exhibited significantly faster LAMP2A degradation rates compared to early-passage cells, we found that lysosomal membranes from late-passage fibroblasts also showed markedly lower levels of phosphorylated LAMP2A than those from early-passage cells (PBP Fig. 18a-c).

To further test whether CMA dysfunction in aging-like models can be rescued by enhancing LAMP2A phosphorylation, we introduced LAMP2A-WT, a non-phosphorylatable mutant (LAMP2A-3A), or a phosphorylation-mimic mutant (LAMP2A-3D) into MRC-5 fibroblasts. Strikingly, expression of LAMP2A-WT or LAMP2A-3D, but not LAMP2A-3A, significantly reduced the senescence-associated β-galactosidase (SA-β-gal) positive cells burden in late-passage fibroblasts (PBP Fig. 18d, e). Critically, this rescue was accompanied by a decrease in known CMA substrates (MEF2D and GAPDH) in whole-cell lysates and their concurrent accumulation in lysosomal fractions, demonstrating enhanced CMA-mediated substrate degradation (PBP Fig. 18f-h). These results suggest that phosphorylation-dependent stabilization of LAMP2A is a conserved mechanism across cell types and that introducing the phosphomimic LAMP2A version (LAMP2A-3D) can ameliorate CMA dysfunction in aging-like models.

We acknowledge that further validation *in vivo* and in other cell types will strengthen these conclusions. However, our data provide evidence for the broad relevance of LAMP2A phosphorylation in CMA regulation.

These Data were included in the updated Supplementary Fig. 3k-p, with detailed descriptions provided on page 14, line 285-300 of the revised manuscript. The newly developed experimental protocol has been incorporated into the Methods section (SA-β-gal staining) on page 52, line 1110-1116).

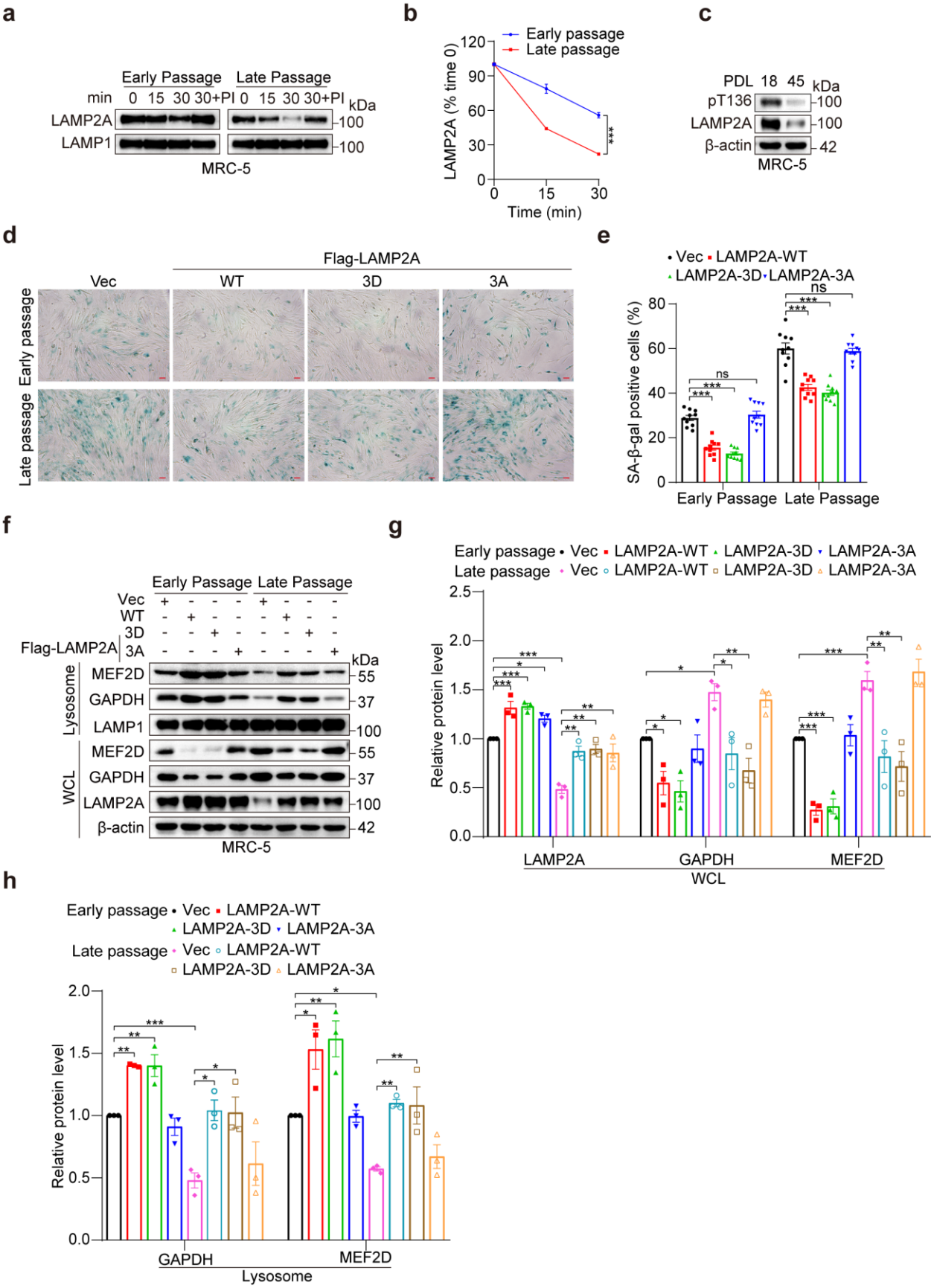
a
Early Passage
Late Passage
min 0 15 30 30+PI 0 15 30 30+PI kDa
LAMP2A -100
LAMP1 -100
MRC-5
b
Early passage
Late passage
LAMP2A (% time 0)
Time (min)
c
PDL 18 45 kDa
pT136 -100
LAMP2A -100
β-actin -42
MRC-5
d
Flag-LAMP2A
Vec
WT
3D
3A
Early passage
Late passage
e
Vec LAMP2A-WT
LAMP2A-3D LAMP2A-3A
SA-β-gal positive cells (%)
Early Passage Late Passage
f
Early Passage Late Passage
Vec
WT
3D
3A
Flag-LAMP2A
kDa
Lysosome
MEF2D -55
GAPDH -37
LAMP1 -100
WCL
MEF2D -55
GAPDH -37
LAMP2A -100
β-actin -42
MRC-5
g
Early passage Vec LAMP2A-WT LAMP2A-3D LAMP2A-3A
Late passage Vec LAMP2A-WT LAMP2A-3D LAMP2A-3A
Relative protein level
LAMP2A
GAPDH
MEF2D
WCL
h
Early passage Vec LAMP2A-WT
LAMP2A-3D LAMP2A-3A
Late passage Vec LAMP2A-WT
LAMP2A-3D LAMP2A-3A
Relative protein level
GAPDH
MEF2D
Lysosome

**PBP Fig. 18 a, b:** Assessment of LAMP2A stability in lysosomes isolated from MRC-5 of early (P18) and late (P45) passage. Lysosomes were incubated at 0℃ for 10 minutes with or without a protease inhibitor (PI), followed by pelleting at indicated time points. LAMP2A and LAMP1 levels were analyzed through immunoblotting, with densitometric quantification of LAMP2A shown in b. Data are presented as the means ± S.E.M. n = 3 independent experiments.

**PBP Fig. 18 c:** IB analyses for indicated proteins in MRC-5 cells of early (P18) and late (P45) passages. PDL, population doubling level.

**PBP Fig. 18 d:** Representative images of senescence-associated beta-galactosidase (SA-β-gal) staining of MRC-5 cells at early (P18) and late (P45) passage with or without overexpressing Flag-LAMP2A-WT/3D/3A. Scale bar, 50 μm.

**PBP Fig. 18 e:** Quantification analyses of the proportion of SA-β-gal positive MRC-5 cells with indicated modifications. Data are presented as the means ± S.E.M. n = 10 randomly selected microscopic fields.

**PBP Fig. 18 f:** IB analyses for indicated proteins in WCL and lysosomal fractions from MRC-5 cells at early (P18) and late (P45) passage with or without overexpressing Flag-LAMP2A-WT/3D/3A.

**PBP Fig. 18 g, h:** Band intensities of indicated proteins were quantified using Image J software, normalized to β-actin levels. Data are presented as the means ± S.E.M. n = 3 independent experiments.

Statistical significance was assessed using two-way ANOVA with Bonferroni's multiple comparisons test (**b**) or one-way ANOVA with Dunnett's multiple comparisons test (**e**, **g**, **h**). ns, not significant. *$p < 0.05$, **$p < 0.01$, ***$p < 0.001$.

8. *During the whole manuscript, authors are trying to point out the relevance of CMA for GSC tumorigenicity and proliferative potential. They are trying to prove that by performing several in vitro and in vivo analysis with different lines of human GSC. Nevertheless, when they test in the in vivo model if LAMP2A or MTS4 regulation in tumor cells changes the immune response to the tumor (Figure 7), they use GB mouse cells, even if they have the tools to do it with the modified GSC. They also use GB mouse cells when studying the effects of IR therapy and anti-PD1 therapy in the in vivo model (Figure 10). Authors should show the results of immune regulation effects with the human GCS lines with the corresponding genetic modifications.*

**Response:** Thank you for this insightful suggestion. We fully recognize the significance of validating immune-modulatory effects in human glioma stem cells (GSCs) and have addressed this through additional experiments. Human GSCs are unable to engraft in immunocompetent C57BL/6 mice due to species-specific barriers, such as a lack of HLA compatibility. Consequently, we employed syngeneic murine GL261 and CT-2A glioma cell lines for our *in vivo* immunotherapy studies (revised Figures 6, 8, and 9).

To directly investigate CMA-mediated immunomodulation within human systems, we conducted *in vitro* co-cultures of modified GSC cell lines (MST4-KD and LAMP2A-KD) with allogeneic human $CD8^+$ T cells. After 48-72 hours of activation using anti-CD3/CD28 beads, T cells are co-cultured with GSC cells at a 1:5 ratio for 24 hours. Flow cytometry analysis revealed that depletion of LAMP2A or MST4 significantly enhanced cytotoxic T-cell responses, as evidenced by increased polyfunctional cytokine production (TNF-α MFI: $0.42\times10^3$ or $0.44\times10^3$ vs. $0.25\times10^3$ in sh-C; $p < 0.001$; IFN-γ MFI: $3.76\times10^3$ or $4.86\times10^3$ vs. $1.39\times10^3$ in sh-C; $p < 0.001$), elevated effector

degranulation production (Granzyme B mean fluorescence intensity: MFI = 0.83×10² or 0.81×10² vs. 0.62 ×10² in sh-C; $p < 0.01$), and increased apoptosis among GSCs (Annexin V⁺PI⁺ cells: 67.10% or 75 .13% vs 52 .70 % in sh-C; $p < 0.01$) (PBP Fig. 19a-d). These findings from human cell data align with observations made from murine tumor models (Supplementary Figure 6g-l), demonstrating an evolutionary conservation of CMA's role in immune evasion.

Although the validation through humanized models remains an important direction for future research, our *in vitro* co-culture experiments indicate that CMA contributes to the functional impairment of CD8⁺ T lymphocytes.

The updated Fig. 6b-d and Supplementary Fig. 6f presents these findings, which are further explained on page 21, line 439-444 and Methods section (page 48, line 1016-1035).

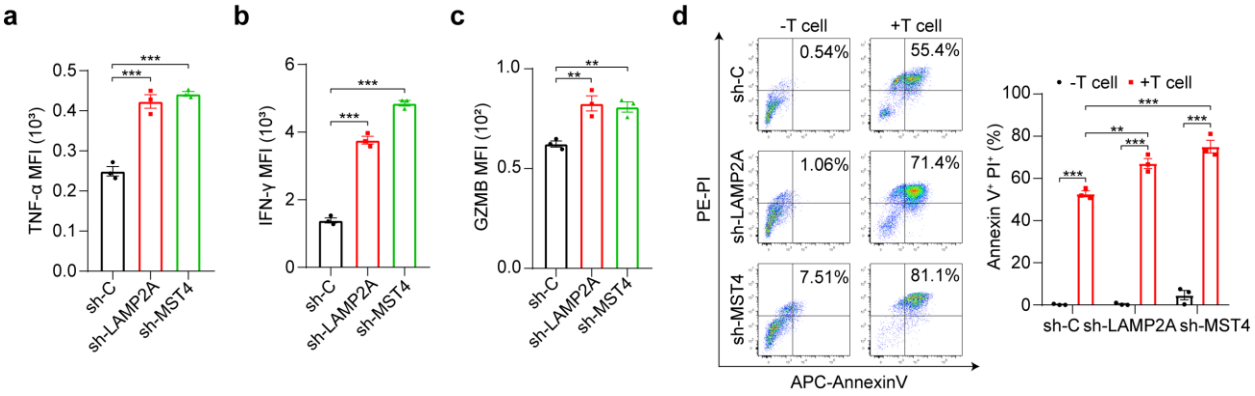


**PBP Fig. 19 a-d:** GSC M83 cells with indicated modification were co-cultured for 24 hours with or without CD8⁺ T cells isolated from GBM patients' peripheral blood. Flow cytometry quantified T cell-derived: TNF-α (**a**), IFN-γ (**b**) and GZMB (**c**) production, as well as Apoptosis analysis of GSC M83 cells (**d**).Data are presented as the mean ± S.E.M. n = 3 independent experiments. MFI, mean fluorescence intensity. PI, propidium iodide.

Statistical significance was assessed using one-way ANOVA with Dunnett's multiple comparisons test (**a-c**) or one-way ANOVA with Tukey's multiple comparisons test (**d**). $^{**}p < 0.01$, $^{***}p < 0.001$.

*9. The inhibitor PPD is used arbitrarily and without context. To improve the quality of the work, authors should show the link, if any, between the phosphorylation of LAMP2A and the modulation of the CMA activity by PPD.*

**Response:** We sincerely appreciate the reviewer's insightful suggestion regarding the mechanistic relationship between LAMP2A phosphorylation and PPD-mediated CMA modulation. In response to this valuable comment, we have conducted additional experiments to elucidate this connection.

As shown in a recent study (Dong RF, et al. *Br J Pharmacol*. 2025), Polyphyllin D (PPD) functions as a selective CMA inhibitor through dual mechanisms: (1) interference with HSC70-LAMP2A interaction and (2) suppression of LAMP2A multimerization. Given that MST4-mediated phosphorylation of LAMP2A promotes its multimerization—an essential step for CMA activation—we explored the impact of PPD on LAMP2A phosphorylation, multimerization, HSC70-LAMP2A interaction, and overall CMA activity.

Our additional experimental results demonstrate:

1) Co-immunoprecipitation and western blot assays revealed that while PPD effectively disrupts the binding between HSC70 and LAMP2A, leading to a decrease in lysosomal association of CMA substrates (TSC1/2, TET3, MEP2D) and an increase in their expression in whole cell lysate (PBP Fig. 20a).
2) PPD does not appear to affect the phosphorylation of LAMP2A (PBP Fig. 20a).
3) Native PAGE analysis provided direct evidence that PPD significantly inhibits LAMP2A multimerization (PBP Fig. 20b)
4) Quantitative photoactivatable CMA reporter assays consistently showed PPD-induced reduction in cellular CMA activity (PBP Fig. 20c, d)

In light of PPD's inhibitory impact on the multimerization of LAMP2A, a downstream consequence of LAMP2A phosphorylation, we employed PPD as a potential inhibitor to interfere with LAMP2A homo-multimerization and subsequently CMA activity.

These Data were shown in revised Supplementary Fig. 8d-g, with detailed descriptions provided on page 26, line 539-550, as well as page 28, line 601-604.

PPD has been identified as a CMA-targeting inhibitor (Dong, Rui-Fang et al. *Br J Pharmacol*. 2025;182(10):2287-2309.); however, its selectivity may be compromised due to its potential impact on alternative cellular stress pathways (Wang, Yang et al. *Mol Ther*. 2023;31(7):2169-2187.). These limitations of PPD have been discussed in the revised manuscript (page 34, line 721-727).

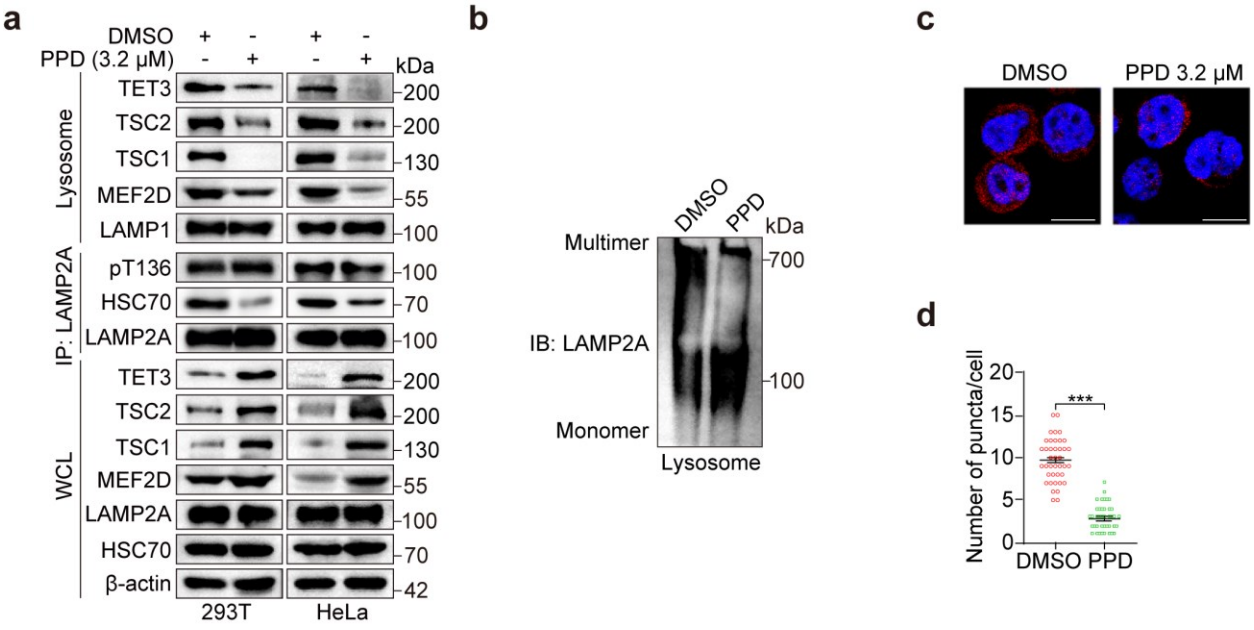


**PBP Fig.20 a:** IP-IB analyses for indicated proteins in WCL and IB analyses for indicated proteins in lysosomal fractions of HEK293T and HeLa cells with or without 3.2 μM PPD treatment.

**PBP Fig.20 b:** Purified lysosomes from the indicated HEK293T cells with or without 3.2 μM PPD treatment were analyzed using native continuous gel electrophoresis and subjected to IB detection for LAMP2A.

**PBP Fig.20 c, d:** Representative images (**c**) and quantification (**d**) of CMA activity detection by KFERQ puncta numbers in GSC M83 cells with or without 3.2 μM PPD treatment. Data are presented as the means ± S.E.M. n = 40 randomly selected cells. Scale bar, 10 μm. Statistical significance was assessed using two-tailed Student's t-test. ***$p < 0.001$.

*10. Supplementary Fig. 1E-H- Authors show some redundant analyses, previously published by other authors (Auzmendi-Iriarte et al., 2022) DOI: 10.1158/0008-5472.CAN-21-2161*

**Response:** Thank you for your suggestion. We have removed Supplementary Figure S1E-H from the revised manuscript, as some redundant analyses previously reported by Auzmendi-Iriarte et al. (2022) (DOI: 10.1158/0008-5472.CAN-21-2161).

*11.Introduction. Authors should enhance the quality of the documentation for the work since their claims are poorly substantiated. Fox example, authors state in line 72 that "the regulatory mechanisms and 73 physiological roles of CMA remain poorly understood", which shows a lack of documentation for the study. To improve the introduction section, they could add different works and reviews on the physiological significance of CMA (doi:10.1038/s41580-018-0001-6; doi:10.1007/978-1-59745-157-4_15)*

**Response:** To improve the introduction, we have added key literature on page 4, line 72, citing important reviews that discuss the physiological roles of CMA (doi:10.1038/s41580-018-0001-6; doi:10.1007/978-1-59745-157-4_15). These additions clarify the regulatory mechanisms and physiological functions of CMA, strengthening the relevance of our study.

*12· Results. Authors claim to have significant differences in several results that are not quantified and are not clear. They also do not explain why they treat lysosomes with just protease inhibitors and they do not add also lysosomal inhibitors such as NH4CL. They also do not really check the glycosylation status of LAMP2A despite having the tools to do so. In addition, all the brain sections shown are at different depths, so they are not comparable.*

**Response:** We sincerely appreciate the reviewer's insightful critiques, which have significantly strengthened our study. Below we provide a point-by-point response to the concerns raised:

1) We apologize for the lack of statistical clarity in the original manuscript. To address this issue, we have reviewed the text and all figures, and provided p-values for all instances of "significant differences" in the figure legends (e.g., Fig. 4b-d).

2) We sincerely appreciate the reviewer's insightful suggestion regarding lysosomal protease inhibition. In our investigation of lysosomal LAMP2A stability and CMA substrate binding/uptake, we employed a protease inhibitor cocktail (10 μM leupeptin, 10 mM AEBSF, 1 mM pepstatin, 100 mM EDTA) to specifically block lysosomal proteolytic activity. This approach effectively prevented luminal degradation of LAMP2A or CMA substrates while maintaining lysosomal integrity, following established CMA research protocols (Juste & Cuervo, *Methods Mol Biol.* 2019). Notably, we excluded $NH_4Cl$ from our purified lysosome

experiments despite its known lysosomal pH-neutralizing effects, as recent evidence suggests it may cause lysosomal membrane damage (Zhang H., et al. *Nat Cell Biol*. 2024;26(11):1892-1902.).

These clarifications have been added to the updated manuscript (page 8, line 162-163), and the revised methods for Immunoblot (IB) analysis (page 45, line 958-964) and *in vitro* lysosome binding and uptake assays (page 51, line 1093-1095).

3) We thank the reviewer for their valuable suggestion. We evaluated the glycosylation status of LAMP2A through PNGase F treatment and Concanavalin A (ConA) blotting, as detailed in the Methods section, followed by immunoblot analysis. LAMP2A was immunoprecipitated using an anti-LAMP2A antibody. After PNGase F treatment, the molecular weight of LAMP2A monomers in both GSC and DGC decreased from about 100 kDa to approximately 50 kDa, indicating complete deglycosylation. The similar sizes of the LAMP2A monomers post-treatment suggest that GSCs and DGCs have comparable glycosylation patterns. Additionally, ConA blotting results showed similar glycosylation levels of LAMP2A in both GSCs and DGCs (PBP Fig. 21 a).

These findings were presented in revised Supplementary Fig. 2a and discussed on page 8-9, line 168-174 of the updated manuscript. PNGase F treatment and Lectin blotting have been added to the revised methods on page 54, line 1144-1158.

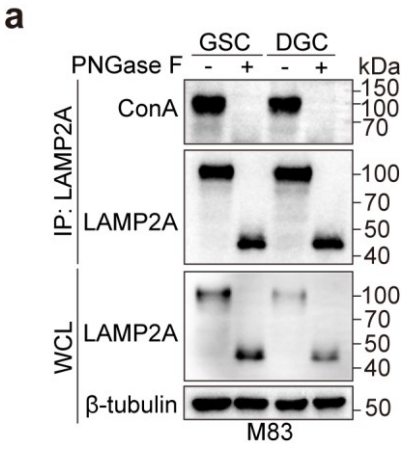


**PBP Fig. 21 a:** IP-IB analyses for LAMP2A and Concanavalin A (ConA) in GSC and DGC M83 cells with or without PNGase F treatment.

4) We thank the reviewer for their detailed assessment and acknowledge the variability in histology sampling. In our tumorigenicity studies, we stereotactically injected different cell lines—5 × $10^4$ GSC M83 cells, 5 × $10^5$ GSC 23 cells, or 1 × $10^5$ GL261 cells—into BALB/c Nude or C57BL/6 mice using standardized coordinates: 2.5 mm lateral, 1.5 mm anterior, and 3.0 mm deep from the skull surface. Coronal sections of the entire brains were prepared at a thickness of 10 μm with a cryostat (Leica), covering the entire rostral-caudal axis of each tumor. We conducted serial section analysis to identify the slice with the largest tumor area for measurement. Due to the invasive nature of the xenografted GBM tumors, they were found at varying depths in the brain sections. To ensure consistency in tumor volume comparisons, we reviewed all tumor sections within each group and selected a comparable

depth for representative H&E-stained sections, then recalculated the tumor volumes of the GBM brain xenografts (PBP Fig. 22 a-f). These data have been updated to the revised Figures 3g-h, 4o-p, and 6h-i.

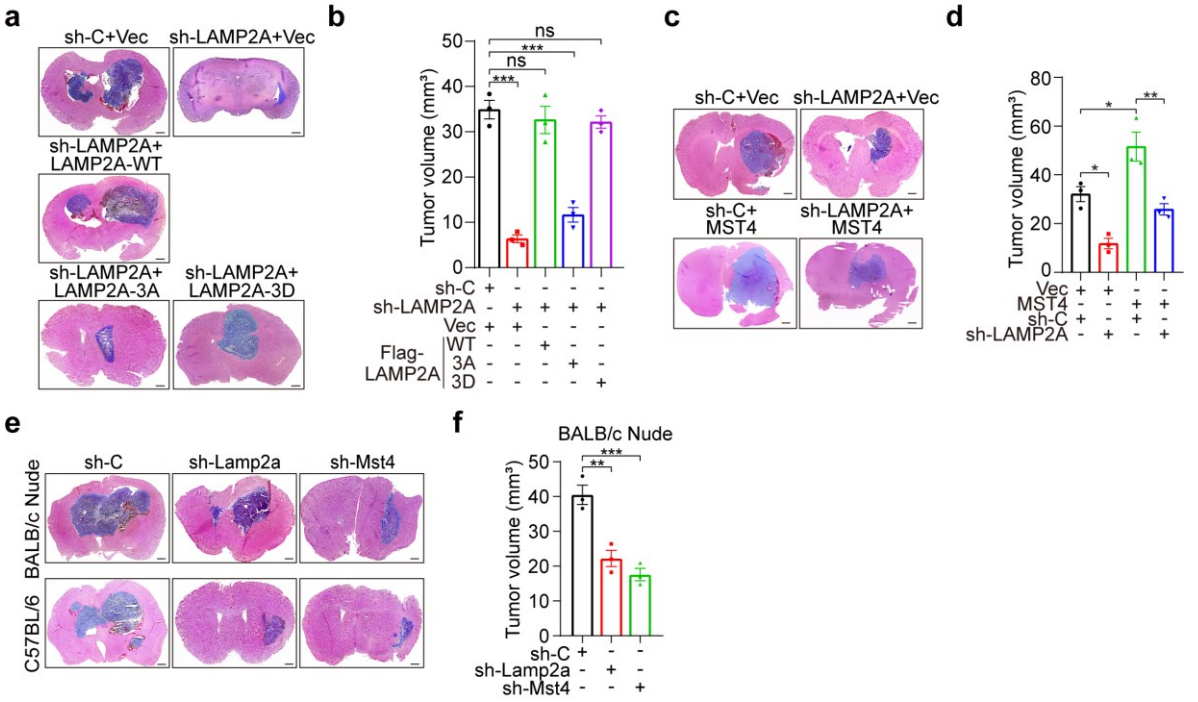


**PBP Fig. 22 a-f:** Representative H&E images and quantitative analysis of tumor volume from athymic (BALB/c Nude) mice or C57BL/6 mice intracranially implanted with GSC M83 cells (**a**, **c**) or GL261 cells (**e**) with indicated modifications. Data are presented as the mean ± S.E.M. n = 3. Scale bar, 1.0 mm. Statistical significance was assessed using one-way ANOVA with Dunnett's multiple comparisons test. ns, not significant. *$p$ < 0.05, **$p$ < 0.01, ***$p$ < 0.001.

*13. Results, line 106. The explanation of the CMA photo-activable reporter is not correct.*

**Response:** We sincerely apologize for the imprecise description of the CMA reporter system. Line 106 in the Results section (now updated to line 103-108 on page 5-6) has been revised to accurately describe the CMA photo-activatable reporter (KFERQ-PA-mCherry). We used this reporter to visualize and quantify CMA activity by counting the fluorescent puncta per cell. This occurs when the fluorescent CMA substrate protein, fused with a KFERQ-like motif, is delivered to CMA-active lysosomes by HSC70, resulting in a transition from a diffuse to a punctate distribution (*Nat Commun*. 2011; 2:386. doi: 10.1038/ncomms1393).

*14. Results, line 112. Authors mention CMA substrates that are not addressed in the text.*

**Response:** We appreciate the reviewer's insightful comment. In the page 6, line 113 of the revised manuscript, we have now provided explicit citations in the revised manuscript (Page 6, Line 114) to substantiate that both MEF2D (*Science*. 2009;323(5910):124-7.) and GAPDH (*J Biol Chem*. 1993;268(14):10463-70.) are well-established CMA substrates in the literature.

*15. Results, line 117. The description of the results obtained in Fig 1c does not match what is observed in the figure. The expression of MEF2D and GAPDH seems to be altered with the different inhibitors.*

**Response:** We appreciate the reviewer's careful observation. In the revised Fig. 1c (PBP Fig. 23a), we have repeated the experiments and included all Western blot replicates for clarity. The results demonstrate that in GSCs, lysosomal inhibition using lysosomal protease inhibitors (leupeptin and ammonium chloride ($NH_4Cl$), LN) significantly increased the levels of CMA substrates (MEF2D and GAPDH), whereas this effect was not observed in conventional GBM cells. In contrast, neither macroautophagy inhibition (3-MA) nor proteasomal inhibition (MG132) altered MEF2D or GAPDH expression. We have corrected the Fig. 1c (page 6, line 111-118) to accurately reflect these findings.

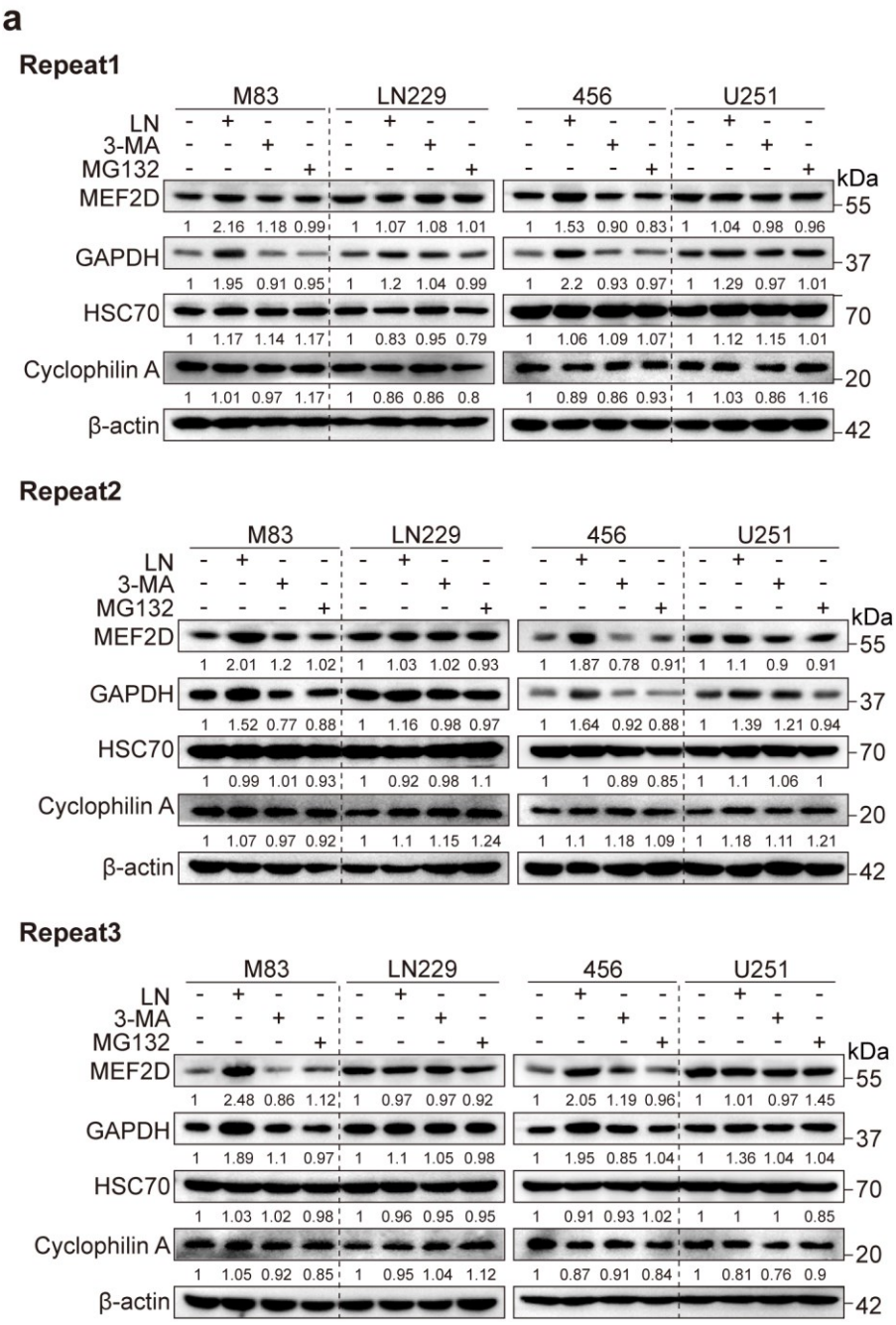


**PBP Fig. 23 a:** IB analyses for indicated proteins after treating with 10 μM MG132, 5 mM 3-MA or, LN (10 μM leupeptin and 20 mM $NH_4Cl$) in GSC cell lines (M83 and 23) and non-GSC cell lines (LN229 and U251), respectively. Band intensities of indicated proteins were quantified using Image J, normalized to β-actin. n = 3 independent experiments.

*16. Results, line 294. Authors cannot state with only an Immunoprecipitation, what effects there may be on CMA activity.*

**Response:** We sincerely appreciate the reviewer's insightful comment regarding the need for additional evidence to support the effects on CMA activity. In response to this concern, we have now conducted additional experiments to further validate our findings. Specifically, we have included: (1) quantification of KFERQ-positive puncta as a direct measure of CMA activity (PBP Fig. 24 a); (2) analysis of lysosomal binding and uptake of GAPDH, a well-established CMA substrate (PBP Fig. 24 b); and (3) examination of MEF2D lysosomal association (PBP Fig. 24 c). These new data collectively provide multiple lines of evidence demonstrating that MST4 indeed enhances CMA activity through LAMP2A. We believe these additional experiments have adequately addressed the reviewer's concern and strengthened our conclusions.

These data were included in the updated Fig. 4i-l, and the revised text now more accurately reflects these experimental validations (page 16, line 324-331 in the revised manuscript).

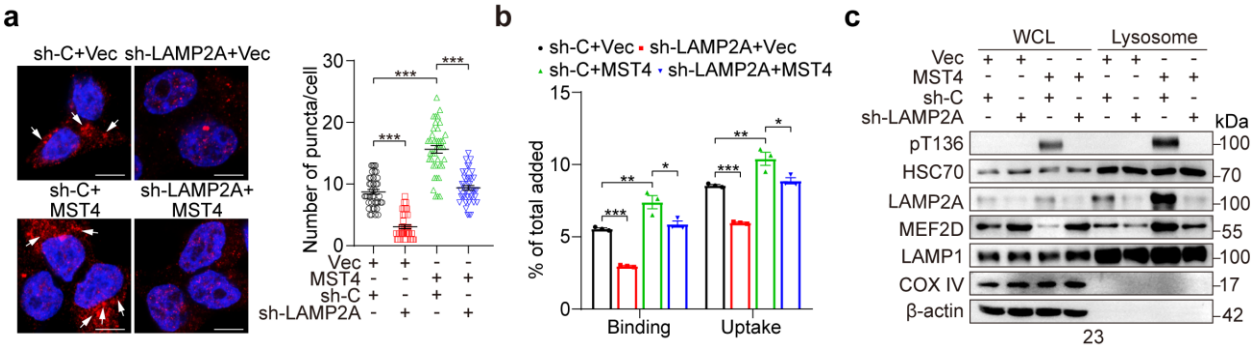


**PBP Fig. 24 a:** Representative images (left) and quantification (right) of CMA activity detection by KFERQ puncta numbers in GSC 23 cells with indicated modifications. Data are presented as the means ± S.E.M. n = 40 randomly selected cells. Scale bar, 10 μm.

**PBP Fig. 24 b:** *In vitro* binding and uptake assay of GAPDH by the lysosome in GSC 23 cells with indicated modifications. Data are presented as the means ± S.E.M. n = 3 independent experiments.

**PBP Fig. 24 c:** IP-IB analyses for indicated proteins in WCL and IB analyses for indicated proteins in lysosomal fractions of GSC 23 cells with indicated modifications.

Statistical significance was assessed using one-way ANOVA with Tukey's multiple comparisons test. ns, not significant. *$p < 0.05$, *$p < 0.01$, ***$p < 0.001$.

***Minor points:***

*17. Results, line 413. There is a typo.*

**Response:** Thank you for catching the typo. We have corrected this in original line 413 (now updated to page 26, line 544) ("However" → "however") and conducted a full-text review to ensure consistency in capitalization and grammar throughout the manuscript. No additional issues were identified.

*18· Results, line 429. The text and the figures mentioned do not match.*

**Response:** We thank the reviewer for their detailed observations. Upon reviewing the text and figures, we realized that the description of Interferon Beta 1 expression in the original manuscript (line 429), as it was not included in Supplementary Fig. 7e, f (now updated to Supplementary Fig. 8b, c). To address this, we have removed the related text on page 25, line 534-537 of the revised manuscript. Additionally, we have meticulously checked the entire manuscript to ensure the consistency of all cited results and figures.

*19· Results, line 466. Authors do not mention PDL-2 in the text even though it is included in supplementary figure 8a.*

**Response:** We appreciate the reviewer's careful attention to the detail. We apologize for the oversight and have now included a detailed description of the PD-L2 results in the Results section (page 27, line 578-581) to align with the data presented in Supplementary Figure 9a.

*20· Methods. The brain coordinates where the stereotactic procedure was performed should be indicated.*

**Response:** Thank you for your important comment. We have indicated the brain coordinates at which the stereotactic procedure was conducted in the revised Methods section of the Animal Studies (page 40, line 851-853). Tumor cells were injected into the brain of individual mice, using the following coordinates from bregma: 2.5 mm lateral, 1.5 mm anterior, and 3.0 mm deep from the skull.

*21· Figure 5E. They show the images and quantification of tumor volume in mice with shC or shLAMP2A GSC 23, and how the volume increases upon MTS4 upregulation. In the text, describing the results, they indicate that the knock down of LAMP2A in GSC23 (a GSC line with low MTS4 expression) had minimal effects on tumorigenicity of GSCs. However, in the figure, it is shown a clear reduction of the tumor in shLAMP2A with a significant statistical analysis.*

**Response:** We apologize for this confusion. We have revised the text to clarify that sh-LAMP2A significantly reduced tumorigenicity in GSC 23 (page 16, line 331-336 of the revised manuscript), consistent with the data in updated Fig. 4o-p.

*22· Supplementary Figure 3d. In order to verify the antibody T136A specificity, it should be tested in the single and double mutants generated for the study, not only in the 3A mutant.*

**Response:** We sincerely appreciate the reviewer's insightful suggestion. To rigorously validate the specificity of the phospho-T136-LAMP2A antibody, we have now performed additional experiments using single and double mutants, alongside the triple mutant (T136A/T40A/S97A, 3A). As shown in PBP Fig. 25a, the antibody specifically detected phosphorylation in LAMP2A-WT, T40A, S97A, and T40A/S97A under exogenous overexpression conditions. However, it completely failed to recognize the T136A phospho-null mutant (T136A), as well as all mutants containing the T136A substitution (T136A/T40A, T136A/S97A, and 3A). These data conclusively demonstrated the antibody's exclusive specificity for the phosphorylated T136 residue.

The updated results are presented in Supplementary Fig. 3d and described in the Results section on page 13, line 262-266 of the revised manuscripts.

**a**

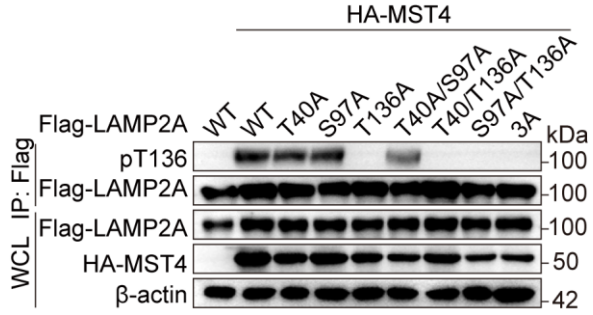


**PBP Fig. 25 a:** IP-IB assessments were conducted for Flag-LAMP2A, HA-MST4, and LAMP2A pT136 in HEK293T cells, both under conditions of MST4 and LAMP2A-WT or -Mut overexpression and in their absence.

*23. Figure 7 and supplementary figure 6. The cytotoxic effect of CD8 T cells should be confirmed with a double staining of CD8 and GZMB to confirm the colocalization. They could perform further analysis to confirm the functionality. In addition, authors could check the reduction of immunosuppressive T cell populations by IHC and by flow cytometry.*

**Response:** We sincerely appreciate the reviewer's insightful suggestion. As recommended, we conducted dual immunofluorescence staining for CD8 (membrane marker) and granzyme B (GZMB, cytotoxic granule marker) in tumor tissues. We found a notable increase in the colocalization of CD8 and GZMB in the tumor tissues of the sh-Mst4 and sh-Lamp2a groups, indicating enhanced cytotoxic activity of $CD8^+$ T cells. (PBP Fig. 26a). In addition, flow cytometry analysis further evaluated the function of infiltrating $CD8^+$ T cells in tumor tissues. In line with the immunofluorescence findings, we observed a significant increase in functionally active $CD8^+$ T cell infiltration within tumors from the sh-Mst4 and sh-Lamp2a groups ($p < 0.001$, PBP Fig. 26b-d). These results reinforce the involvement of CMA in facilitating tumor immune evasion. Representative images and quantitative analysis are provided in revised Supplementary Fig. 6i-l. The updated data were described on page 22, line 456-464 of the revised manuscript.

For assessment of immunosuppressive T cells populations, we performed double staining for CD4 (membrane, red) and FoxP3 (nuclear, green) in tumor sections. Quantitative analysis of $FoxP3^+$ $CD4^+$ cells within tumor regions revealed decreased Tregs infiltration in the sh-Mst4 and sh-Lamp2a groups ($p < 0.001$, PBP Fig. 26e). In addition, we analyzed $FoxP3^+$ $CD4^+$ regulatory

T cells (Tregs) in tumor single-cell suspensions using flow cytometry, and we observed diminished infiltration of Tregs within the tumor microenvironment in the sh-Mst4 and sh-Lamp2a groups ($p < 0.001$, PBP Fig. 26f). These data were included in revised Supplementary Fig. 6h, m, and are described on page 22, line 456-464 of the revised manuscript.

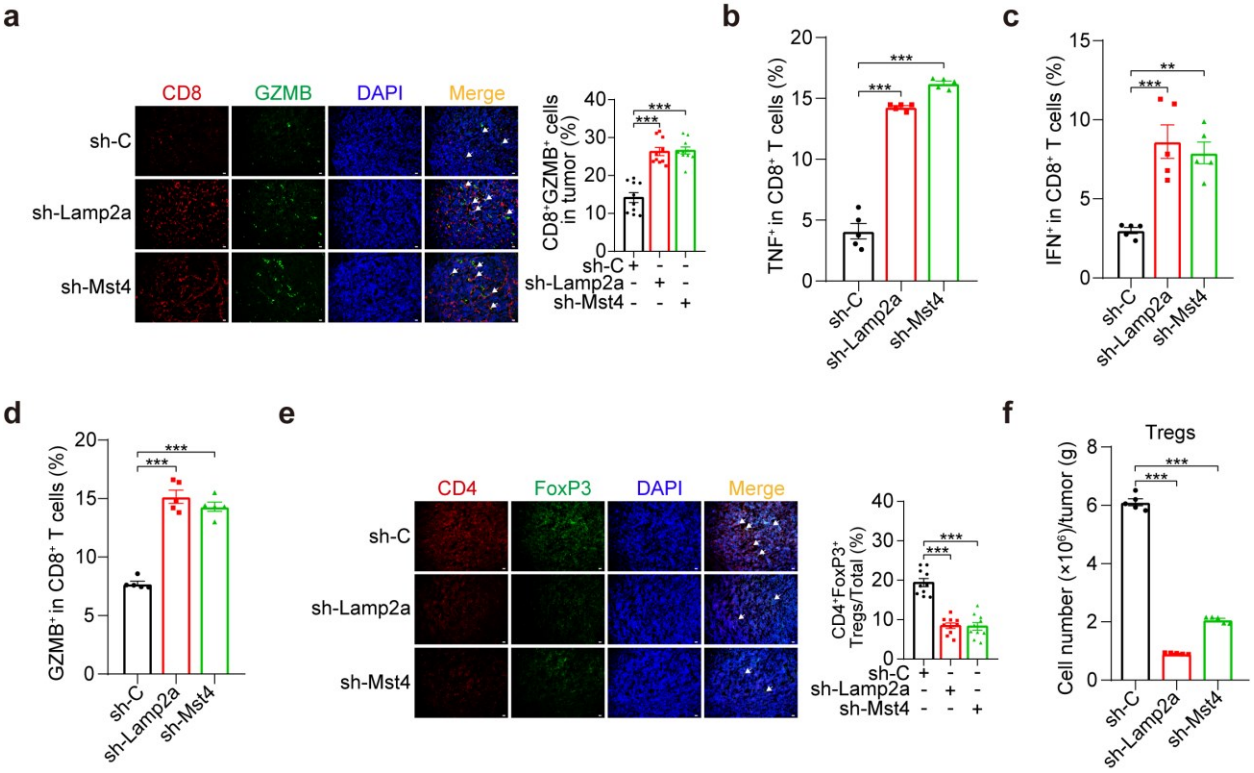


**PBP Fig. 26 a, e:** Representative IF staining images (left) and quantification (right) for $CD8^+$ $GZMB^+$ cells (**a**) and $CD4^+$ $FoxP3^+$ Tregs (**e**) in tumor tissues from C57/BL6 mice with intracranial CT-2A cells transplants with indicated modifications. Data are presented as the means ± S.E.M. n = 10 randomly selected microscopic fields. Scale bar, 20 μm.

**PBP Fig. 26 b-d:** Flow cytometric analysis of population of $TNF^+CD8^+$ T cells (**b**), $IFN^+CD8^+$ T cells (**c**) and $GZMB^+CD8^+$ T cells (**d**) in infiltrating $CD8^+$ T cells from tumor tissues of C57/BL6 mice with intracranial CT-2A cells transplants with indicated modifications. Data are presented as the means ± S.E.M. n = 5 independent experiments.

**PBP Fig. 26 f:** Flow cytometric analyses of population of infiltrating Tregs in tumor tissues from C57/BL6 mice with intracranial CT-2A cells transplants with indicated modifications. Data are presented as the means ± S.E.M. n = 5 independent experiments.

Statistical significance was assessed using one-way ANOVA with Dunnett's multiple comparisons test (**a-f**). $^{**}p < 0.01$, $^{***}p < 0.001$.

*24. Figure 11. An IHC analysis of GB patient samples is shown as well as a correlation analysis between the studied markers. In material and methods, authors describe that they have defined a score in order to perform the correlation analysis between the high and low expression of the*

*markers. Nevertheless, the ranges the use for high and low expression are not well stablished. For instance, a sample with a score of 3 or 4 could be high and low at the same time according to their criteria. In addition, it is not mentioned in the text.*

**Response:** We re-evaluated the quantitative scoring of tissue section staining based on the percentage of positively stained cells and staining intensity (PBP Fig. 27a, b), adhering to established protocols (*Nat Cell Biol.* 2022;24(11):1655-1665; *Nature*. 2011;480(7375):118-22.). The scoring was as follows: 0 for 0% positive tumor cells, 1 for 0–1%, 2 for 2–10%, 3 for 11–30%, 4 for 31–70%, and 5 for 71–100%. Staining intensity was rated from 0 to 3, with 0 indicating negative, 1 weak, 2 moderate, and 3 strong. The total score, ranging from 0 to 8, was calculated by combining the proportion and intensity scores. We compared these scores with overall survival duration, defined as the time from diagnosis to death or last follow-up. Kaplan-Meier plots were generated for overall survival rates of GBM patients, categorized into high (staining score 4–8) and low (staining score 0–3) expression groups of the indicated protein. These results are included in the updated Fig. 10 b-c and detailed on page 53, line 1124-1134 of the revised methods for IHC analysis of clinical glioma specimens.

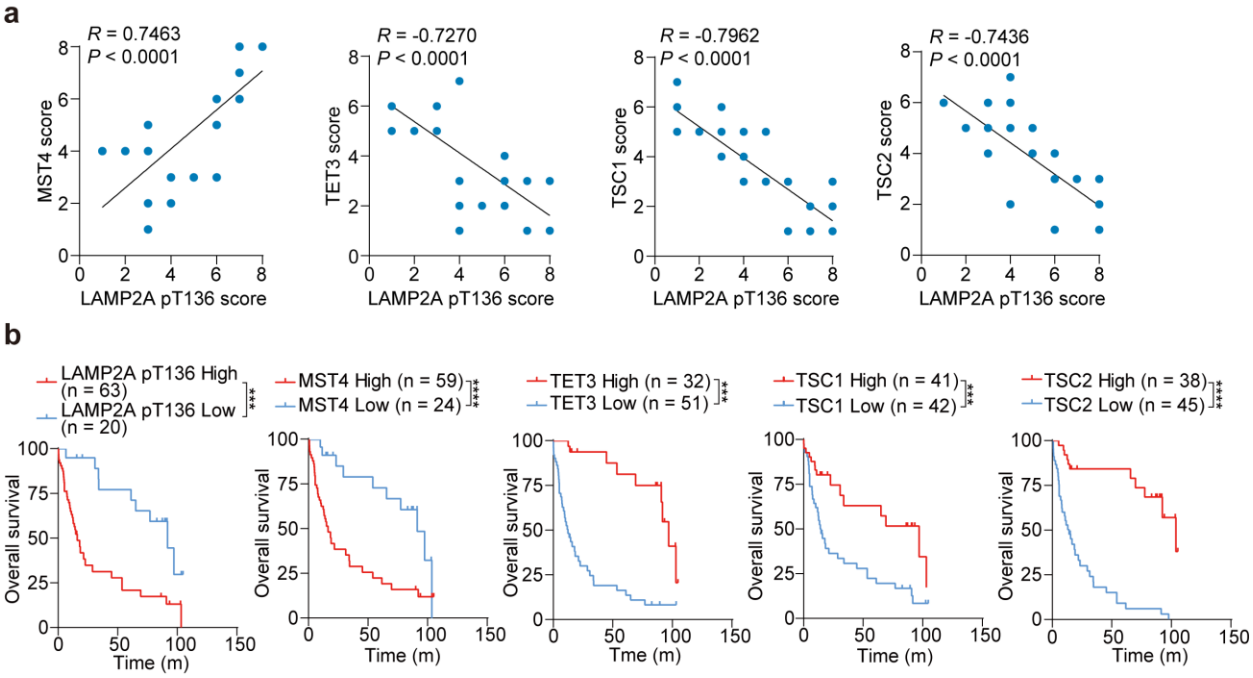


**PBP Fig. 27 a:** Scoring of IHC staining of human glioma samples using the specified antibodies, followed by correlation analysis utilizing a two-tailed Pearson correlation test. n = 83. Note that some sample scores may overlap.

**PBP Fig. 27 b:** Kaplan-Meier survival analyses for glioma patients categorized by high or low expression levels of LAMP2A pT136, MST4, TET3, TSC1 and TSC2. n = 83. IHC score ≥ 4 was considered as high expression samples, IHC score ≤ 3 was considered as low expression samples. Statistical significance was assessed using log-rank test. ***$p < 0.001$.

**Manuscript Number: NCOMMS-25-06239A-Z-R1**

**Point-to-Point Responses to Reviewer's Comments**

We sincerely appreciate the enthusiasm with which the editor and reviewers have engaged with our revised submission. We have thoroughly addressed all of their concerns and questions in this updated manuscript. We believe that the revised version offers a more comprehensive and informative presentation of our research, and we are grateful to the reviewers for their valuable suggestions. Therefore, we are pleased to submit this revised manuscript for further consideration. Below, we provide point-by-point responses to each comment:

***Reviewer #1:***

*The authors have addressed my comments, except the code availability as per Nature communications' guidelines.*

**Response:** We sincerely appreciate the reviewer's constructive feedback and valuable suggestions, which have significantly strengthened the clarity and reproducibility of our manuscript. We regret the oversight regarding code availability in our resubmission and confirm that all relevant code and data access details have been successfully made public via the PRIDE database (https://www.ebi.ac.uk/pride/archive/projects/PXD060464).

We sincerely apologize for any inconvenience caused and deeply appreciate the reviewer's diligence in highlighting this critical requirement. Your feedback has been instrumental in enhancing the rigor and accessibility of our work.

***Reviewer #2:***

*We appreciate and applaud the authors' thoughtful and substantial revisions in response to our prior feedback. The manuscript is now suitable for publication, pending resolution of a few minor comments outlined below.*

**Response:** We thank the reviewer for the enthusiasm and the positive comments. We also appreciate the reviewer's excellent comments and suggestions. We have included further clarification and discussion of limitations to address the reviewer's concerns in our revised manuscript.

*Minor Comments:*

*1- Clarification of CMA Marker Interpretation:*

*Page 6, Results, Line: 104-116:*

*The authors quite effectively demonstrate increased CMA activity in GSCs compared to non-GSCs with the PA-mCherry-KFERQ reporter. For clarity, however, it would be helpful to include*

*a brief description of how puncta per cell reflects CMA activity and to differentiate this measurement from general lysosomal activity, given the centrality of this assay*

**Response:** We sincerely appreciate the reviewer's insightful feedback regarding the interpretation of CMA activity in our study. We have added a brief description of how puncta per cell reflects CMA activity and to differentiate this measurement from general lysosomal activity in the revised manuscript (Page 7, Lines 106–108).

*2- Expanded Discussion on CMA Regulation:*

*Page 9-10, Line: 180-194:*

*The authors well demonstrate MST4-LAMP2A interactions in conditions of stress (IR and starvation). Perhaps mention in brief the overall implications of this stress-induced interaction within the tumor microenvironment, such as how it may regulate GSC behavior in vivo under conditions of hypoxia or starvation commonly encountered within GBM tumors.*

**Response:** We sincerely appreciate the reviewer's insightful suggestion regarding the broader implications of MST4-LAMP2A interactions within the tumor microenvironment. In response to this valuable feedback, we have incorporated a brief discussion on the overall implications of stress-induced MST4-LAMP2A interactions in the tumor microenvironment in the revised manuscript (Page 11, Lines 194-197).

*3- Lysosomal Protease Inhibition Consistency:*

*Page 8, Lines: 156-163 (Methods in Rebuttal response, Minor Comment 5):*

*Authors detailed in the rebuttal the explicit use of a protease inhibitor cocktail other than the LN (leupeptin/NH4Cl). However, a transitional mention in main manuscript methods or figure legends would raise transparency and methodological clarity in the light of the nuanced difference between LN and the more general PI cocktail.*

**Response:** We sincerely appreciate the reviewer's suggestion regarding methodological transparency. To address this concern, we have taken the following steps:

**Methodological Clarification**: We have now added a transitional statement in the Methods section (Page 47, Lines 981-984; Page 54, Lines 1117-1118) explicitly stating: "For CMA activity assays, a protease inhibitor cocktail (containing 10 μM leupeptin (targeting serine/cysteine proteases), 10 μM AEBSF (serine protease inhibitor), 1 μM pepstatin A (aspartic protease inhibitor), and 100 μM EDTA (metalloprotease inhibitor)) was used instead of leupeptin/$NH_4Cl$ to specifically inhibit lysosomal proteases while minimizing interference with CMA machinery."

**Figure Legend Update**: In relevant figure legends, we have included: "protease inhibitor cocktail (PI) to inhibit lysosomal protease activity" (Page 9, Line 163; Page 12, Line 215; Page 20, Line 396; Page 69, Lines 1629-1633; Line 8, Supplementary Figure 7 legend; Line 11, Supplementary Figure 10 legend).

We appreciate this suggestion as it improves the methodological rigor of our study. The changes have been made consistently across all relevant experimental descriptions.

*4- Depth of Immunophenotyping in Syngeneic Models:*

*The authors have been able to address previous reviewer recommendations regarding the immunological mechanisms of CMA modulation. An inclusion of a short discussion sentence in the revised manuscript acknowledging the potential role of other significant immune cells beyond CD8+ T cells (Tregs, MDSCs, TAMs), although briefly, would provide a complete immunological perspective, especially since potential future research might venture into exploring these avenues.*

**Response:** We sincerely appreciate the insightful suggestions provided by the reviewer. In response to this significant point, we have incorporated a brief discussion in the revised manuscript (Page 35, Lines 725-728), which states: "While our study primarily focuses on $CD8^+$ T cells, we acknowledge that other immune cell populations, including Tregs, MDSCs, and TAMs, may also participate in CMA-mediated immune modulation within the tumor microenvironment."

***Reviewer #4:***

*In the revised version, the new experiments added, provide evidence that TCS1/2 and TET3 are CMA substrates in human GSCs and could be used as therapeutic targets. However, there is not yet a clear link between the described mechanism and the inhibitor used. Additionally, several major points needs to be addressed so that the work meets the standards of the journal.*

**Response:** We sincerely appreciate the reviewer's insightful comments and constructive suggestions, which have significantly strengthened our manuscript. Below we provide point-by-point responses to each concern, with all recommended revisions implemented.

*1. The authors state in the introduction that "the specific role of CMA in these cells [GSCs] is yet to be elucidated", and in the first results section, they conclude that "these result//s indicated that CMA is required for GSC stemness and tumorigenicity". However, these results are just a validation of the study already published in 2022 by Auzmendi-Iriarte et al. (doi.org/10.1158/0008-5472.CAN-21-2161). Although they could include these results as supplementary material to give context to the subsequent analysis of LAMP2A stability in the lysosomes of GSCs, the authors of this paper cannot include the first section of results as novel. In addition, they should elaborate further in the introduction and discussion on the work of Auzmendi-Iriarte et al. to expand the information. Overall, the authors should restructure the article in detail to actually report the mechanism they are describing.*

**Response:** We sincerely appreciate the reviewer's valuable feedback. To address these comments, we have substantially expanded the discussion of Auzmendi-Iriarte et al.'s important work in both the Introduction (Page 5, Lines 68-72) and Discussion (Pages 33-34, Lines 681-686) sections. Concurrently, we have adjusted the strength of our claims regarding CMA's role in GSC stemness and tumorigenicity to more accurately reflect the current evidence.

*2. With the new experiments provided, the authors show that the inhibitor PPD does not affect the phosphorylation state of LAMP2A and that it inhibits its multimerization (Supplementary Fig. 8d-g). However, these results increase the lack of connection between the MST4-LAMP2A regulation and the use of PPD in the study. The results obtained with the inhibitor PPD both in vitro and in vivo are very promising, but do not justify why the authors have included this inhibitor in their therapeutical strategies when, apparently, it has no relevance on the described mechanism. It would be more appropriate for authors to submit the work to an autophagy journal, as without a specific inhibitor with effect on the in vivo models, the described regulatory mechanism lacks translational impact.*

**Response:** We sincerely appreciate the reviewer's insightful critique regarding the mechanistic connection between MST4-LAMP2A regulation and our use of PPD inhibitor. In response to these important comments, we would like to clarify the following points:

1. PPD is identified as an inhibitor of chaperone-mediated autophagy (CMA) that acts by preventing the multimerization of LAMP2A (Dong, Rui-Fang et al. *Br J Pharmacol*. 2025;182(10):2287-2309). Although PPD does not directly influence LAMP2A phosphorylation (Supplementary Fig. 11d-g), it inhibits LAMP2A multimerization, a downstream consequence of MST4-LAMP2A signaling in CMA. Our data show that knocking down MST4 or using a phospho-null LAMP2A mutant (3A) significantly blocks LAMP2A multimerization (Fig. 2k, Supplementary Fig. 3g), demonstrating that PPD functions similarly to MST4 inhibition or preventing LAMP2A phosphorylation.

2. Given our *in vitro* findings that radiation significantly increases MST4 expression and enhances the MST4-LAMP2A interaction (Supplementary Fig. 2i), radiation therapy should similarly elevate MST4 expression and strengthen the MST4-LAMP2A interaction *in vivo*. This enhanced interaction would promote LAMP2A phosphorylation, multimerization, and ultimately increase CMA activity in *in vivo* models. Since PPD effectively inhibits LAMP2A multimerization—a downstream consequence of LAMP2A phosphorylation—we investigated the effects of this CMA inhibitor when combined with radiation therapy and anti-PD-1 monoclonal antibody (mAb) treatment in the GL261 and CT-2A C57BL/6 intracranial glioblastoma (GBM) models. Further studies are required to determine whether PPD suppresses CMA activity by inhibiting radiation-induced LAMP2A multimerization in *in vivo* models.

3. We have revised the manuscript to include a discussion on the limitations of PPD as a CMA inhibitor. Additionally, we have proposed future investigations into more selective CMA-targeting inhibitors, such as CIM7, to enhance our therapeutic strategies and translational impact (Page 36, Lines 732-740).

We are grateful for the opportunity to strengthen these aspects of our work and appreciate the reviewer's constructive feedback.

3. *In the response to reviewers' comments, the authors state that they have not been able to perform the in vivo model with human GSC lines because "human GSCs are unable to engraft in immunocompetent C57BL/6 mice due to species-specific barriers". However, they have also not tried the different therapeutic strategies in BALB/c nude mice that could perfectly well develop human GSCs tumors. In addition, there are other authors who have used human glioblastoma cells lines to develop a tumor in immunocompetent mice (Molina et al., 2022, doi.org/10.3389/fcell.2022.797945; Garcia et al., 2014, doi.org/10.1186/1471-2407-14-923).*

*Therefore, without the in vivo experiments using human glioma cells the study lacks the translational impact necessary to get the standars of Nature Communications.*

**Response:** We are deeply grateful for the reviewer's thoughtful comments regarding the utilization of human GSC models in immunocompetent murine systems. Our preliminary investigations with multiple human GSC lines in C57BL/6 mice demonstrated an inability to establish tumors in immunocompetent hosts, consistent with established species-specific barriers. To address this technical constraint, we developed sophisticated *in vitro* co-culture platforms interrogating human GSC-$CD8^+$ T cell interactions. Quantitative flow cytometric analyses revealed that genetic perturbation of either LAMP2A or MST4 significantly augmented cytotoxic T lymphocyte responses, as demonstrated by: (1) enhanced polyfunctional cytokine production (TNF-α, Fig. 6b; IFN-γ, Fig. 6c), (2) elevated effector molecule expression (Granzyme B, Fig. 6d), and (3) increased GSC apoptosis (Supplementary Fig. 9f).

These limitations and future directions have been addressed in the revised Discussion section (Page 35-36, Lines 728-732). The reviewer's constructive critique has substantially strengthened our experimental framework and will undoubtedly inform subsequent translational studies.

*4. Although the authors have followed the request to include papers on the physiological significance of CMA, they have not updated the introduction in accordance with the new works cited.*

**Response:** We sincerely appreciate the reviewer's valuable feedback regarding the inclusion of recent literature on CMA's physiological significance. In response to this constructive suggestion, we have now cited two of the most recent studies on CMA' s physiological significance (Reynolds CA et al., PNAS, 2024; Khawaja RR et al., Nature Aging, 2025) in the Introduction section.

*5. Fig. 5A- Authors show some redundant analyses, previously published by Auzmendi-Iriarte et al., 2022 (doi.org/10.1158/0008-5472.CAN-21-2161), which are the original source of the RNAseq study used.*

**Response:** Thank you for your insightful feedback regarding the analyses presented in Fig. 5A. We acquired the GSE181556 dataset (Auzmendi-Iriarte et al., 2022) and utilized the normalized expression matrix to analyze LAMP2A-associated signaling pathways using Gene Set Enrichment Analysis (GSEA). The original study by Auzmendi-Iriarte et al. (2022, doi: 10.1158/0008-5472.CAN-21-2161) employed RNAseq analysis based on the Kyoto Encyclopedia of Genes and Genomes (KEGG) pathway framework. We have now explicitly cited this foundational work in the revised manuscript (Page 18, Lines 356-358) and clearly specified the RNAseq data source in the Methods section (Page 44, Line 902).